

# 1 Anthropogenic Secondary Organic Aerosols Contribute Substantially to Air Pollution 2 Mortality

3

4 Benjamin A. Nault<sup>1,2,\*</sup>, Duseong S. Jo<sup>1,2</sup>, Brian C. McDonald<sup>2,3</sup>, Pedro Campuzano-Jost<sup>1,2</sup>, Douglas A.  
5 Day<sup>1,2</sup>, Weiwei Hu<sup>1,2,\*\*</sup>, Jason C. Schroder<sup>1,2,\*\*\*</sup>, James Allan<sup>4,5</sup>, Donald R. Blake<sup>6</sup>, Manjula R.  
6 Canagaratna<sup>7</sup>, Hugh Coe<sup>5</sup>, Matthew M. Coggon<sup>2,3</sup>, Peter F. DeCarlo<sup>8</sup>, Glenn S. Diskin<sup>9</sup>, Rachel  
7 Dunmore<sup>10</sup>, Frank Flocke<sup>11</sup>, Alan Fried<sup>12</sup>, Jessica B. Gilman<sup>3</sup>, Georgios Gkatzelis<sup>2,3,\*\*\*\*</sup>, Jacqui F.  
8 Hamilton<sup>10</sup>, Thomas F. Hanisco<sup>13</sup>, Patrick L. Hayes<sup>14</sup>, Daven K. Henze<sup>15</sup>, Alma Hodzic<sup>11,16</sup>, James  
9 Hopkins<sup>10,17</sup>, Min Hu<sup>18</sup>, L. Gregory Huey<sup>19</sup>, B. Thomas Jobson<sup>20</sup>, William C. Kuster<sup>3,\*\*\*\*\*</sup>, Alastair  
10 Lewis<sup>10,17</sup>, Meng Li<sup>2,3</sup>, Jin Liao<sup>13,21</sup>, M. Omar Nawaz<sup>15</sup>, Ilana B. Pollack<sup>22</sup>, Jeffrey Peischl<sup>2,3</sup>, Bernhard  
11 Rappenglück<sup>23</sup>, Claire E. Reeves<sup>24</sup>, Dirk Richter<sup>12</sup>, James M. Roberts<sup>3</sup>, Thomas B. Ryerson<sup>3,\*\*\*\*\*</sup>, Min  
12 Shao<sup>25</sup>, Jacob M. Sommers<sup>14,26</sup>, James Walega<sup>12</sup>, Carsten Warneke<sup>2,3</sup>, Petter Weibring<sup>12</sup>, Glenn M.  
13 Wolfe<sup>13,27</sup>, Dominique E. Young<sup>5,\*\*\*\*\*</sup>, Bin Yuan<sup>25</sup>, Qiang Zhang<sup>28</sup>, Joost A. de Gouw<sup>1,2</sup>, and Jose L.  
14 Jimenez<sup>1,2,+</sup>

15

16 1. Department of Chemistry, University of Colorado, Boulder, Boulder, CO, USA

17 2. Cooperative Institute for Research in Environmental Sciences, Boulder, Colorado, USA

18 3. Chemical Sciences Division, NOAA Earth System Research Laboratory, Boulder, CO

19 4. National Centre for Atmospheric Sciences, School of Earth and Environmental Sciences, University of Manchester, Manchester, UK

20 5. Centre of Atmospheric Science, School of Earth and Environmental Sciences, University of Manchester, Manchester, UK

21 6. Department of Chemistry, University of California, Irvine, Irvine, CA, USA

22 7. Center for Aerosol and Cloud Chemistry, Aerodyne Research Inc., Billerica, MA, USA

23 8. Department of Environmental Health Engineering, Johns Hopkins University, Baltimore, MD, USA

24 9. NASA Langley Research Center, Hampton, Virginia, USA

25 10. Wolfson Atmospheric Chemistry Laboratories, Department of Chemistry, University of York, York, UK

26 11. Atmospheric Chemistry Observations and Modeling Laboratory, National Center for Atmospheric Research, Boulder, CO, USA

27 12. Institute of Arctic and Alpine Research, University of Colorado, Boulder, CO, USA

28 13. Atmospheric Chemistry and Dynamic Laboratory, NASA Goddard Space Flight Center, Greenbelt, MD, USA

29 14. Department of Chemistry, Université de Montréal, Montréal, QC, Canada

30 15. Department of Mechanical Engineering, University of Colorado, Boulder, CO, USA

31 16. Laboratoires d'Aréologie, Université de Toulouse, CNRS, UPS, Toulouse, France

32 17. National Centre for Atmospheric Sciences, Department of Chemistry, University of York, York, UK

33 18. State Key Joint Laboratory of Environmental Simulation and Pollution Control, College of Environmental Sciences and Engineering, Peking

34 University, Beijing, China

35 19. School of Earth and Atmospheric Sciences, Georgia Institute of Technology, Atlanta, Georgia, USA

36 20. Laboratory for Atmospheric Research, Department of Civil and Environmental Engineering, Washington State University, Pullman, WA,

37 USA

38 21. Universities Space Research Association, GESTAR, Columbia, MD, USA

39 22. Department of Atmospheric Science, Colorado State University, Fort Collins, CO, USA

40 23. Department of Earth and Atmospheric Science, University of Houston, Houston, TX, USA

41 24. Centre for Ocean and Atmospheric Sciences, School of Environmental Sciences, University of East Anglia, Norwich, UK

42 25. Institute for Environmental and Climate Research, Jinan University, Guangzhou, China

43 26. Air Quality Research Division, Environment and Climate Change Canada, Toronto, Ontario, Canada

44 27. Joint Center for Earth Systems Technology, University of Maryland, Baltimore County, Baltimore, MD, USA

45 28. Ministry of Education Key Laboratory for Earth System Modeling, Department of Earth System Science, Tsinghua University, Beijing, China

46 \*Now at Center for Aerosol and Cloud Chemistry, Aerodyne Research Inc., Billerica, MA, USA

47 \*\*Now at State Key Laboratory at Organic Geochemistry, Guangzhou Institute of Geochemistry, Chinese Academy of Sciences, Guangzhou,

48 China

49 \*\*\*Now at Colorado Department of Public Health and Environment, Denver, CO, USA

50 \*\*\*\*Now at Forschungszentrum Juelich GmbH, Juelich, Germany

51 \*\*\*\*\*Has retired and worked on this manuscript as an unaffiliated co-author.

52 \*\*\*\*\*Now at Scientific Aviation, Boulder, CO, USA

53 \*\*\*\*\*Now at Air Quality Research Center, University of California, Davis, CA, USA

54

55

56 +Corresponding author: Jose L. Jimenez ([jose.jimenez@colorado.edu](mailto:jose.jimenez@colorado.edu))

57

## 58 **Abstract**

59 Anthropogenic secondary organic aerosol (ASOA), formed from anthropogenic emissions of  
60 organic compounds, constitutes a substantial fraction of the mass of submicron aerosol in  
61 populated areas around the world and contributes to poor air quality and premature mortality.  
62 However, the precursor sources of ASOA are poorly understood, and there are large uncertainties  
63 in the health benefits that might accrue from reducing anthropogenic organic emissions. We  
64 show that the production of ASOA in 11 urban areas on three continents is strongly correlated  
65 with the reactivity of specific anthropogenic volatile organic compounds. The differences in  
66 ASOA production across different cities can be explained by differences in the emissions of  
67 aromatics and intermediate- and semi-volatile organic compounds, indicating the importance of  
68 controlling these ASOA precursors. With an improved modeling representation of ASOA driven  
69 by the observations, we attribute 340,000  $PM_{2.5}$  premature deaths per year to ASOA, which is  
70 over an order of magnitude higher than prior studies. A sensitivity case with a more recently  
71 proposed model for attributing mortality to  $PM_{2.5}$  (the Global Exposure Mortality Model) results  
72 in up to 900,000 deaths. A limitation of this study is the extrapolation from cities with detailed  
73 studies and regions where detailed emission inventories are available to other regions where  
74 uncertainties in emissions are larger. In addition to further development of institutional air  
75 quality management infrastructure, comprehensive air quality campaigns in the countries in  
76 South and Central America, Africa, South Asia, and the Middle East are needed for further  
77 progress in this area.

## 78 **1. Introduction**

79 Poor air quality is one of the leading causes of premature mortality worldwide (Cohen et  
80 al., 2017; Landrigan et al., 2018). Roughly 95% of the world's population live in areas where  
81  $PM_{2.5}$  (fine particulate matter with diameter smaller than 2.5  $\mu m$ ) exceeds the World Health  
82 Organization's 10  $\mu g m^{-3}$  annual average guideline (Shaddick et al., 2018). This is especially true  
83 for urban areas, where high population density is co-located with increased emissions of  $PM_{2.5}$   
84 and its gas-phase precursors from human activities. It is estimated that  $PM_{2.5}$  leads to 3 to 4  
85 million premature deaths per year, higher than the deaths associated with other air pollutants  
86 (Cohen et al., 2017). More recent analysis using concentration-response relationships derived  
87 from studies of populations exposure to high levels of ambient  $PM_{2.5}$  suggest the global  
88 premature death burden could be up to twice this value (Burnett et al., 2018).

89 The main method to estimate premature mortality with  $PM_{2.5}$  is to use measured  $PM_{2.5}$   
90 from ground observations along with derived  $PM_{2.5}$  from satellites to fill in missing ground-based  
91 observations (van Donkelaar et al., 2015, 2016). To go from total  $PM_{2.5}$  to species-dependent and  
92 even sector-dependent associated premature mortality from  $PM_{2.5}$ , chemical transport models  
93 (CTMs) are used to predict the fractional contribution of species and/or sector (e.g., Lelieveld et  
94 al., 2015; van Donkelaar et al., 2015, 2016; Silva et al., 2016). However, though CTMs may get  
95 total  $PM_{2.5}$  or even total species, e.g., organic aerosol (OA), correct, the model may be getting the  
96 values right for the wrong reason (e.g., de Gouw and Jimenez, 2009; Woody et al., 2016; Murphy  
97 et al., 2017; Baker et al., 2018; Hodzic et al., 2020). This is especially important for OA in urban  
98 areas, where models have a longstanding issue under predicting secondary OA (SOA) with some  
99 instances of over predicting primary OA (POA) (de Gouw and Jimenez, 2009; Dzepina et al.,

100 2009; Hodzic et al., 2010b; Woody et al., 2016; Zhao et al., 2016a; Janssen et al., 2017; Jathar et  
101 al., 2017). Further, this bias has even been observed for highly aged aerosols in remote regions  
102 (Hodzic et al., 2020). As has been found in prior studies for urban areas (e.g., Zhang et al., 2007;  
103 Kondo et al., 2008; Jimenez et al., 2009; DeCarlo et al., 2010; Hayes et al., 2013; Freney et al.,  
104 2014; Hu et al., 2016; Nault et al., 2018; Schroder et al., 2018) and highlighted here (Fig. 1), a  
105 substantial fraction of the observed submicron PM is OA, and a substantial fraction of the OA is  
106 composed of SOA (approximately a factor of 2 to 3 higher than POA). Thus, to better understand  
107 the sources and apportionment of  $PM_{2.5}$  that contributes to premature mortality, CTMs must  
108 improve their prediction of SOA versus POA, as the sources of SOA precursors and POA can be  
109 different.

110         However, understanding the gas-phase precursors of photochemically-produced  
111 anthropogenic SOA (ASOA, defined as the photochemically-produced SOA formed from the  
112 photooxidation of anthropogenic volatile organic compounds (AVOC) (de Gouw et al., 2005;  
113 DeCarlo et al., 2010)) quantitatively is challenging (Hallquist et al., 2009). Note, for the rest of  
114 the paper, unless explicitly stated otherwise, ASOA refers to SOA produced from the  
115 photooxidation of AVOCs, as there are potentially other relevant paths for the production of SOA  
116 in urban environments (e.g., Petit et al., 2014; Kodros et al., 2018, 2020; Stavroulas et al., 2019).  
117 Though the enhancement of ASOA is largest in large cities, these precursors and production of  
118 ASOA should be important in any location impacted by anthropogenic emissions (e.g., Fig. 1).  
119 ASOA comprises a wide range of condensable products generated by numerous chemical  
120 reactions involving AVOC precursors (Hallquist et al., 2009; Hayes et al., 2015; Shrivastava et  
121 al., 2017). The number of AVOC precursors, as well as the role of “non-traditional” AVOC

122 precursors, along with the condensable products and chemical reactions, compound to lead to  
123 differences in the observed versus predicted ASOA for various urban environments (e.g., de  
124 Gouw and Jimenez, 2009; Dzepina et al., 2009; Hodzic et al., 2010b; Woody et al., 2016; Janssen  
125 et al., 2017; Jathar et al., 2017; McDonald et al., 2018). One solution to improve the prediction in  
126 CTMs is to use a simplified model, where lumped ASOA precursors react, non-reversibly, at a  
127 given rate constant, to produce ASOA (Hodzic and Jimenez, 2011; Hayes et al., 2015; Pai et al.,  
128 2020). This simplified model has been found to reproduce the observed ASOA from some urban  
129 areas (Hodzic and Jimenez, 2011; Hayes et al., 2015) but issues in other urban areas (Pai et al.,  
130 2020). This may stem from the simplified model being parameterized to two urban areas (Hodzic  
131 and Jimenez, 2011; Hayes et al., 2015). These inconsistencies impact the model predicted  
132 fractional contribution of ASOA to total  $PM_{2.5}$  and thus the ability to understand the source  
133 attribution to  $PM_{2.5}$  and premature deaths.

134         The main categories of gas-phase precursors that dominate ASOA have been the subject  
135 of intensive research. The debate on what dominates can in turn impact the understanding of  
136 what precursors to regulate to reduce ASOA, to improve air quality, and to reduce premature  
137 mortality associated with ASOA. Transportation-related emissions (e.g., tailpipe, evaporation,  
138 refueling) were assumed to be the major precursors of ASOA, which was supported by field  
139 studies (Parrish et al., 2009; Gentner et al., 2012; Warneke et al., 2012; Pollack et al., 2013). Yet,  
140 budget closure of observed ASOA mass concentrations could not be achieved with  
141 transportation-related VOCs (Ensberg et al., 2014). The contribution of urban-emitted biogenic  
142 precursors to SOA in urban areas is typically small. Biogenic SOA (BSOA) in urban areas  
143 typically results from advection of regional background concentrations rather than processing of

144 locally emitted biogenic VOCs (e.g., Hodzic et al., 2009, 2010a; Hayes et al., 2013; Janssen et  
145 al., 2017). BSOA is thought to dominate globally (Hallquist et al., 2009), but as shown in Fig. 1,  
146 the contribution of BSOA (1% to 20%) to urban concentrations, while often substantial, is  
147 typically smaller than that of ASOA (17% to 39%) (see Sect. S3.1).

148 Many of these prior studies generally investigated AVOC with high volatility, where  
149 volatility here is defined as the saturation concentration,  $C^*$ , in  $\mu\text{g m}^{-3}$  (de Gouw et al., 2005;  
150 Volkamer et al., 2006; Dzepina et al., 2009; Freney et al., 2014; Woody et al., 2016). More recent  
151 studies have identified lower volatility compounds in transportation-related emissions (e.g., Zhao  
152 et al., 2014, 2016b; Lu et al., 2018). These compounds have been broadly identified as  
153 intermediate-volatile organic compounds (IVOCs) and semi-volatile organic compounds  
154 (SVOCs). IVOCs have a  $C^*$  generally of  $10^3$  to  $10^6 \mu\text{g m}^{-3}$  while SVOCs have a  $C^*$  generally of  
155  $1$  to  $10^2 \mu\text{g m}^{-3}$ . Due to their lower volatility and functional groups, these classes of compounds  
156 generally form ASOA more efficiently than traditional, higher volatile AVOCs; however,  
157 S/IVOCs have also been more difficult to measure (e.g., Zhao et al., 2014; Pagonis et al., 2017;  
158 Deming et al., 2018). IVOCs generally have been the more difficult of the two classes to measure  
159 and identify as these compounds cannot be collected onto filters to be sampled off-line (Lu et al.,  
160 2018) and generally show up as unresolved complex mixture for in-situ measurements using  
161 gas-chromatography (GC) (Zhao et al., 2014). SVOCs, on the other hand, can be more readily  
162 collected onto filters and sampled off-line due to their lower volatility (Lu et al., 2018). Another  
163 potential issue has been an under-estimation of the S/IVOC aerosol production, as well as an  
164 under-estimation in the contribution of photochemically produced S/IVOC from photooxidized  
165 “traditional” VOCs, due to partitioning of these low volatile compounds to chamber walls and

166 tubing (Krechmer et al., 2016; Ye et al., 2016; Liu et al., 2019). Accounting for this  
167 under-estimation increases the predicted ASOA (Ma et al., 2017). The inclusion of these classes  
168 of compounds have led to improvement in some urban SOA budget closure; however, many  
169 studies still have indicated a general short-fall in ASOA budget even when including these  
170 compounds from transportation-related emissions. (Dzepina et al., 2009; Tsimpidi et al., 2010;  
171 Hayes et al., 2015; Cappa et al., 2016; Ma et al., 2017; McDonald et al., 2018).

172         Recent studies have indicated that emissions from volatile chemical products (VCPs),  
173 defined as pesticides, coatings, inks, adhesives, personal care products, and cleaning agents  
174 (McDonald et al., 2018), as well as cooking emissions (Hayes et al., 2015), asphalt emissions  
175 (Khare et al., 2020), and solid fuel emissions from residential wood burning and/or cookstoves  
176 (e.g., Hu et al., 2013, 2020; Schroder et al., 2018), are important. While total amounts of ASOA  
177 precursors released in cities have dramatically declined (largely due to three-way catalytic  
178 converters in cars (Warneke et al., 2012; Pollack et al., 2013; Zhao et al., 2017; Khare and  
179 Gentner, 2018)), VCPs have not declined as quickly (Khare and Gentner, 2018; McDonald et al.,  
180 2018). Besides a few cities in the US (Coggon et al., 2018; Khare and Gentner, 2018; McDonald  
181 et al., 2018), extensive VCP emission quantification has not yet been published.

182         Due to the uncertainty on the emissions of ASOA precursors and on the amount of  
183 ASOA formed from them, the number of premature deaths associated with urban organic  
184 emissions is largely unknown. Since numerous studies have shown the importance of VCPs and  
185 other non-traditional VOC emission sources, efforts have been made to try to improve the  
186 representation and emissions of VCPs (Seltzer et al., 2021), which can reduce the uncertainty in  
187 ASOA precursors and the associated premature deaths estimations. Currently, most studies have



188 not included ASOA realistically (e.g., Lelieveld et al., 2015; Silva et al., 2016; Ridley et al.,  
189 2018) in source apportionment calculations of the premature deaths associated with long-term  
190 exposure of  $PM_{2.5}$ . These models represented total OA as non-volatile POA and “traditional”  
191 ASOA precursors (transportation-based VOCs), which largely under-predict ASOA (Ensberg et  
192 al., 2014; Hayes et al., 2015; Nault et al., 2018; Schroder et al., 2018) while over-predicting POA  
193 (e.g., Hodzic et al., 2010b; Zhao et al., 2016a; Jathar et al., 2017). This does not reflect the  
194 current understanding that POA is volatile and contributes to ASOA mass concentration (e.g.,  
195 Grieshop et al., 2009; Lu et al., 2018). Though the models are estimating total OA correctly  
196 (Ridley et al., 2018; Hodzic et al., 2020; Pai et al., 2020), the attribution of premature deaths to  
197 POA instead of SOA formed from “traditional” and “non-traditional” sources, including IVOCs  
198 from both sources, could lead to regulations that may not target the emissions that would reduce  
199 OA in urban areas. As  $PM_1$  and SOA mass are highest in urban areas (Fig. 1), also shown in  
200 Jimenez et al. (2009), it is necessary to quantify the amount and identify the sources of ASOA to  
201 target future emission standards that will optimally improve air quality and the associated health  
202 impacts. As these emissions are from human activities, they will contribute to SOA mass outside  
203 urban regions and to potential health impacts outside urban regions as well. Though there are  
204 potentially other important exposure pathways to PM that may increase premature mortality,  
205 such as exposure to solid-fuel emissions indoors (e.g., Kodros et al., 2018), the focus of this  
206 paper is on exposure to outdoor ASOA and its associated impacts to premature mortality.

207         Here, we investigate the factors that control ASOA using 11 major urban, including  
208 megacities, field studies (Fig. 1 and Table 1). The empirical relationships and numerical models  
209 are then used to quantify the attribution of premature mortality to ASOA around the world, using

210 the observations to improve the modeled representation of ASOA. The results provide insight  
211 into the importance of ASOA to global premature mortality due to  $PM_{2.5}$  and further  
212 understanding of the precursors and sources of ASOA in urban regions.

213

## 214 **2. Methods**

215 Here, we introduce the ambient observations from various campaigns used to constrain  
216 ASOA production (Sect. 2.1), description of the simplified model used in CTMs to better predict  
217 ASOA (Sect. 2.2), and description of how premature mortality was estimated for this study (Sect.  
218 2.3). In the SI, the following can be found: description of the emissions used to calculate the  
219 ASOA budget for five different locations (Sect. S1), description of how the ASOA budget was  
220 calculated for the five different locations (Sect. S2), description of the CTM (GEOS-Chem) used  
221 in this study (Sect. S3 - S4), and error analysis for the observations (Sect. S5).

222

### 223 **2.1 Ambient Observations**

224 For values not previously reported in the literature (Table S4), observations taken  
225 between 11:00 – 16:00 local time were used to determine the slopes of SOA versus  
226 formaldehyde (HCHO) (Fig. S1), peroxy acetyl nitrate (PAN) (Fig. S2), and  $O_x$  ( $O_x = O_3 + NO_2$ )  
227 (Fig. S3). For CalNex, there was an approximate 48% difference between the two HCHO  
228 measurements (Fig. S4). Therefore, the average between the two measurements were used in this  
229 study, similar to what has been done in other studies for other gas-phase species (Bertram et al.,  
230 2007). All linear fits, unless otherwise noted, use the orthogonal distance regression fitting  
231 method (ODR).

232 For values in Table S4 through Table S8 not previously reported in the literature, the  
 233 following procedure was applied to determine the emissions ratios, similar to the methods of  
 234 Nault et al. (2018). An OH exposure ( $OH_{exp} = [OH] \times \Delta t$ ), which is also the photochemical age  
 235 (PA), was estimated by using the ratio of  $NO_x/NO_y$  (Eq. 1) or the ratio of  
 236 m+p-xylene/ethylbenzene (Eq. 2). For the m+p-xylene/ethylbenzene, the emission ratio  
 237 (Table S5) was determined by determining the average ratio during minimal photochemistry,  
 238 similar to prior studies (de Gouw et al., 2017). This was done for only one study, TexAQS 2000.  
 239 This method could be applied in that case as it was a ground campaign that operated both day  
 240 and night; therefore, a ratio at night could be determined when there was minimal loss of both  
 241 VOCs. The average emission ratio for the other VOCs was determined using Eq. 3 after the  
 242  $OH_{exp}$  was calculated in Eq. 1 or Eq. 2. The rate constants used for determining  $OH_{exp}$  and  
 243 emission ratios are found in Table S12.

$$244 \quad OH_{exp} = [OH] \times t = \ln \left( \frac{\left( \frac{[NO_x]}{[NO_y]} \right)}{k_{OH+NO_2}} \right) \quad \text{Eq. 1}$$

$$245 \quad OH_{exp} = [OH] \times t = - \frac{1}{k_{m+p-xylene} - k_{ethylbenzene}} \times \ln \left( \frac{[m+p-xylene]_t}{[ethylbenzene]_t} - \frac{[m+p-xylene]_0}{[ethylbenzene]_0} \right) \quad \text{Eq. 2}$$

$$247 \quad \frac{[VOC(i)]}{[CO]}(0) = - \frac{[VOC(i)]}{[CO]}(t) \times \left( 1 - \frac{1}{\exp(-k_i \times [OH]_{exp} \times t)} \right) \times k_i + \frac{[VOC(i)]}{[CO]}(t) \times k_i \quad \text{Eq. 3}$$

249  
 250 **2.2 Updates to the SIMPLE Model**

251 With the combination of the new dataset, which expands across urban areas on three  
252 continents, the SIMPLE parameterization for ASOA (Hodzic and Jimenez, 2011) is updated in  
253 the standard GEOS-Chem model to reproduce observed ASOA in Fig. 2a. The parameterization  
254 operates as represented by Eq. 4.



256 SOAP represents the lumped precursors of ASOA,  $k$  is the reaction rate coefficient with OH  
257 ( $1.25 \times 10^{-11} \text{ cm}^3 \text{ molecules}^{-1} \text{ s}^{-1}$ ), and  $[\text{OH}]$  is the OH concentration in molecules  $\text{cm}^{-3}$ . This rate  
258 constant is also consistent with observed ASOA formation time scale of  $\sim 1$  day that has been  
259 observed across numerous studies (e.g., de Gouw et al., 2005; DeCarlo et al., 2010; Hayes et al.,  
260 2013; Nault et al., 2018; Schroder et al., 2018).

261 SOAP emissions were calculated based on the relationship between  $\Delta\text{SOA}/\Delta\text{CO}$  and  
262  $R_{\text{aromatics}}/\Delta\text{CO}$  in Fig. 2a. First, we calculated  $R_{\text{aromatics}}/\Delta\text{CO}$  (Eq. 5) for each grid cell and time step  
263 as follows:

$$264 \quad \frac{R_{\text{aromatics}}}{\Delta\text{CO}} = \frac{E_{\text{B}} \times k_{\text{B}} + E_{\text{T}} \times k_{\text{T}} + E_{\text{X}} \times k_{\text{X}}}{E_{\text{CO}}} \quad \text{Eq. 5}$$

265 Where  $E$  and  $k$  stand for the emission rate and reaction rate coefficient with OH, respectively, for  
266 benzene (B), toluene (T), and xylenes (X). Ethylbenzene was not included in this calculation  
267 because its emission was not available in HTAPv2 emission inventory. However, ethylbenzene  
268 contributed a minor fraction of the mixing ratio ( $\sim 7\%$ , Table S5) and reactivity ( $\sim 6\%$ ) of the  
269 total BTEX across the campaigns. Reaction rate constants used in this study were  $1.22 \times 10^{-12}$ ,  
270  $5.63 \times 10^{-12}$ , and  $1.72 \times 10^{-11} \text{ cm}^3 \text{ molec.}^{-1} \text{ s}^{-1}$  for benzene, toluene, and xylene, respectively  
271 (Atkinson and Arey, 2003; Atkinson et al., 2006). The  $R_{\text{aromatics}}/\Delta\text{CO}$  allows a dynamic

272 calculation of the  $E(\text{VOC})/E(\text{CO}) = \text{SOA}/\Delta\text{CO}$ . Hodzic and Jimenez (2011) and Hayes et al.  
 273 (2015) used a constant value of  $0.069 \text{ g g}^{-1}$ , which worked well for the two cities investigated,  
 274 but not for the expanded dataset studied here. Thus, both the aromatic emissions and CO  
 275 emissions are used in this study to better represent the variable emissions of ASOA precursors  
 276 (Fig. S5).

277 Second,  $E_{\text{SOAP}}/E_{\text{CO}}$  can be obtained from the result of Eq. 6, using slope and intercept in  
 278 Fig. 2a, with a correction factor (F) to consider additional SOA production after 0.5 PA  
 279 equivalent days, since Fig. 2a shows the comparison at 0.5 PA equivalent days.

$$280 \quad \frac{E_{\text{SOAP}}}{E_{\text{CO}}} = \left( \text{Slope} \times \frac{R_{\text{Aromatics}}}{\Delta\text{CO}} + \text{Intercept} \right) \times F \quad \text{Eq. 6}$$

281 Where slope is 24.8 and intercept is  $-1.7$  from Fig. 2a. F (Eq. 7) can be calculated as follows:

$$282 \quad F = \frac{ASOA_{t=\infty}}{ASOA_{t=0.5d}} = \frac{SOAP_{t=0}}{SOAP_{t=0} \times (1 - \exp(-k \times \Delta t \times [\text{OH}])), \Delta t = 43200 \text{ s}} \quad \text{Eq. 7}$$

283 F was calculated as 1.8 by using  $[\text{OH}] = 1.5 \times 10^6 \text{ molecules cm}^{-3}$ , which was used in the  
 284 definition of 0.5 PA equivalent days for Fig. 2a.

285 Finally,  $E_{\text{SOAP}}$  can be computed by multiplying CO emissions ( $E_{\text{CO}}$ ) for every grid point  
 286 and time step in GEOS-Chem by the  $E_{\text{SOAP}}/E_{\text{CO}}$  ratio.

287

### 288 **2.3 Estimation of Premature Mortality Attribution**

289 Premature deaths were calculated for five disease categories: ischemic heart disease  
 290 (IHD), stroke, chronic obstructive pulmonary disease (COPD), acute lower respiratory illness  
 291 (ALRI), and lung cancer (LC). We calculated premature mortality for the population aged more  
 292 than 30 years, using Eq. 8.

293 
$$Premature\ Death = Pop \times y_0 \times \frac{RR - 1}{RR}$$
 Eq. 8

294 Mortality rate,  $y_0$ , varies according to the particular disease category and geographic region,  
 295 which is available from Global Burden of Disease (GBD) Study 2015 database (IHME, 2016).  
 296 Population (Pop) was obtained from Columbia University Center for International Earth Science  
 297 Information Network (CIESIN) for 2010 (CIESIN, 2017). Relative risk, RR, can be calculated as  
 298 shown in Eq. 9.

299 
$$RR = 1 + \alpha \times \left( 1 - \exp\left(\beta \times \left(PM_{2.5} - PM_{2.5,Threshold}\right)^\rho\right)\right)$$
 Eq. 9

300  $\alpha$ ,  $\beta$ , and  $\rho$  values depend on disease category and are calculated from Burnett et al. (2014) (see  
 301 Table S14 and associated file). If the  $PM_{2.5}$  concentrations are below the  $PM_{2.5}$  threshold value  
 302 (Table S14), premature deaths were computed as zero. However, there could be some health  
 303 impacts at concentrations below the  $PM_{2.5}$  threshold values (Krewski et al., 2009); following the  
 304 methods of the GBD studies, these can be viewed as lower bounds on estimates of premature  
 305 deaths.

306 We performed an additional sensitivity analysis using the Global Exposure Mortality  
 307 Model (GEMM) (Burnett et al., 2018). For the GEMM analysis, we also used age stratified  
 308 population data from GWPv3. Premature death is calculated the same as shown in Eq. 8;  
 309 however, the relative risk differs. For the GEMM model, the relative risk can be calculated as  
 310 shown in Eq. 10.

311 
$$RR = \exp(\theta \times \lambda) \text{ with } \lambda = \frac{\log\left(1 + \frac{z}{\alpha}\right)}{\left(1 + \exp\left(\frac{(\hat{\mu} - z)}{\pi}\right)\right)}$$
 Eq. 10

312 Here  $z = \max(0, PM_{2.5} - PM_{2.5, Threshold})$ ;  $\theta$ ,  $\pi$ ,  $\hat{\mu}$ ,  $\alpha$ , and  $PM_{2.5, Threshold}$  depends on disease category and  
313 are from Burnett et al. (2018). Similar to the Eq. 9, if the concentrations are below the threshold  
314 ( $2.4 \mu\text{g m}^{-3}$ , Burnett et al. (2018)), then premature deaths are computed as zero; however, the  
315 GEMM has a lower threshold than the GBD method.

316 For GBD, we do not consider age-specific mortality rates or risks. For GEMM, we  
317 calculate age-specific health impacts with age-specific parameters in the exposure response  
318 function (Table S15). We combine the age-specific results of the exposure-response function  
319 with age distributed population data from GPW (CIESIN, 2017) and a national mortality rate  
320 across all ages to assess age-specific mortality.

321 We calculated total premature deaths using annual average total  $PM_{2.5}$  concentrations  
322 derived from satellite-based estimates at the resolution of  $0.1^\circ \times 0.1^\circ$  from van Donkelaar et al.  
323 (2016) . Application of the remote-sensing based  $PM_{2.5}$  at the  $0.1^\circ \times 0.1^\circ$  resolution rather than  
324 direct use of the GEOS-Chem model concentrations at the  $2^\circ \times 2.5^\circ$  resolution helps reduce  
325 uncertainties in the quantification of  $PM_{2.5}$  exposure inherent in coarser estimates (Punger and  
326 West, 2013). We also calculated deaths by subtracting from this amount the total annual average  
327 ASOA concentrations derived from GEOS-Chem (Fig. S11). To reduce uncertainties related to  
328 spatial gradients and total concentration magnitudes in our GEOS-Chem simulations of  $PM_{2.5}$ ,  
329 our modeled ASOA was calculated as the fraction of ASOA to total  $PM_{2.5}$  in GEOS-Chem,  
330 multiplied by the satellite-based  $PM_{2.5}$  concentrations (Eq. 11).

$$331 \quad ASOA_{sat} = (ASOA_{mod} / PM_{2.5, mod}) \times PM_{2.5, sat} \quad \text{Eq. 11}$$

332 Finally, this process for estimating  $PM_{2.5}$  health impacts considers only  $PM_{2.5}$  mass concentration  
333 and does not distinguish toxicity by composition, consistent with the current US EPA position  
334 expressed in Sacks et al. (2019).

335

### 336 **3. Observations of ASOA Production across Three Continents**

#### 337 **3.1 Observational Constraints of ASOA Production across Three Continents**

338 Measurements during intensive field campaigns in large urban areas better constrain  
339 concentrations and atmospheric formation of ASOA because the scale of ASOA enhancement is  
340 large compared to SOA from a regional background. Generally, ASOA increased with the  
341 amount of urban precursor VOCs and with atmospheric PA (de Gouw et al., 2005; de Gouw and  
342 Jimenez, 2009; DeCarlo et al., 2010; Hayes et al., 2013; Nault et al., 2018; Schroder et al., 2018;  
343 Shah et al., 2018). In addition, ASOA correlates strongly with gas-phase secondary  
344 photochemical species, including  $O_x$ , HCHO, and PAN (Herndon et al., 2008; Wood et al., 2010;  
345 Hayes et al., 2013; Zhang et al., 2015; Nault et al., 2018; Liao et al., 2019) (Table S4; Fig. S1 to  
346 Fig. S3), which are indicators of photochemical processing of emissions.

347 However, as initially discussed by Nault et al. (2018) and shown in Fig. 3, there is large  
348 variability in these various metrics across the urban areas evaluated here. To the best of the  
349 authors' knowledge, this variability has not been explored and its physical meaning has not been  
350 interpreted. As shown in Fig. 3, though, the trends in  $\Delta SOA/\Delta CO$  are similar to the trends in the  
351 slopes of SOA versus  $O_x$ , PAN, or HCHO. For example, Seoul is the highest for nearly all  
352 metrics, and is approximately a factor of 6 higher than the urban area, Houston, that generally



353 showed the lowest photochemical metrics. This suggests that the variability is related to a  
354 physical factor, including emissions and chemistry.

355 The VOC concentration, together with how quickly the emitted VOCs react ( $\sum k_i \times [\text{VOC}]_i$ ,  
356 i.e., the hydroxyl radical, or OH, reactivity of VOCs), where k is the OH rate coefficient for each  
357 VOC, are a determining parameter for ASOA formation over urban spatial scales (Eq. 12).  
358 ASOA formation is normalized here to the excess CO mixing ratio ( $\Delta\text{CO}$ ) to account for the  
359 effects of meteorology, dilution, and non-urban background levels, and allow for easier  
360 comparison between different studies:

$$361 \quad \frac{\Delta \text{ASOA}}{\Delta \text{CO}} \propto [\text{OH}] \times \Delta t \times \left( \sum_i k_i \times \left[ \frac{\text{VOC}}{\text{CO}} \right]_i \times Y_i \right) \quad \text{Eq. 12}$$

362 where Y is the aerosol yield for each compound (mass of SOA formed per unit mass of precursor  
363 reacted), and  $[\text{OH}] \times \Delta t$  is the PA.

364 BTEX are one group of known ASOA precursors (Gentner et al., 2012; Hayes et al.,  
365 2013), and their emission ratio (to CO) was determined for all campaigns (Table S5). BTEX can  
366 thus provide insight into ASOA production. Fig. 2a shows that the variation in ASOA (at PA =  
367 0.5 equivalent days) is highly correlated with the emission reactivity ratio of BTEX ( $R_{\text{BTEX}}$ ,  
368  $\sum_i [\text{VOC}/\text{CO}]_i$ ) across all the studies. However, BTEX alone cannot account for much of the  
369 ASOA formation (see budget closure discussion below), and instead, BTEX may be better  
370 thought of as both partial contributors and also as indicators for the co-emission of other  
371 (unmeasured) organic precursors that are also efficient at forming ASOA.

372  $\text{O}_x$ , PAN, and HCHO are produced from the oxidation of a much wider set of VOC  
373 precursors (including small alkenes, which do not appreciably produce SOA when oxidized).

374 These alkenes have similar reaction rate constants with OH as the most reactive BTEX  
375 compounds (Table S12); however, their emissions and concentration can be higher than BTEX  
376 (Table S7). Thus, alkenes would dominate  $R_{\text{Total}}$ , leading to  $\text{O}_x$ , HCHO, and PAN being produced  
377 more rapidly than ASOA (Fig. 2b–d). When  $R_{\text{BTEX}}$  becomes more important for  $R_{\text{Total}}$ , the emitted  
378 VOCs are more efficient in producing ASOA. Thus, the ratio of ASOA to gas-phase  
379 photochemical products shows a strong correlation with  $R_{\text{BTEX}}/R_{\text{Total}}$  (Fig. 2b–d).

380 An important aspect of this study is that most of these observations occurred during  
381 spring and summer, when solid fuel emissions are expected to be lower (e.g., Chafe et al., 2015;  
382 Lam et al., 2017; Hu et al., 2020). Further, the most important observations used here are during  
383 the afternoon, investigating specifically the photochemically produced ASOA. These results here  
384 might partially miss any ASOA produced through nighttime aqueous chemistry or oxidation by  
385 nitrate radical (Kodros et al., 2020). However, two of the studies included in our analysis,  
386 Chinese Outflow (CAPTAIN, 2011) and New York City (WINTER, 2015), occurred in late  
387 winter/early spring, when solid fuel emissions were important (Hu et al., 2013; Schroder et al.,  
388 2018). We find that these observations lie within the uncertainty in the slope between ASOA and  
389  $R_{\text{BTEX}}$  (Fig. 2a). Their photochemically produced ASOA observed under strong impact from solid  
390 fuel emissions shows similar behavior as the ASOA observed during spring and summer time.  
391 Thus, given the limited datasets currently available, photochemically produced ASOA is  
392 expected to follow the relationship shown in Fig. 2a and is expected to also follow this  
393 relationship for regions impacted by solid fuel burning. Future comprehensive studies in regions  
394 strongly impacted by solid fuel burning are needed to further investigate photochemical ASOA  
395 production under those conditions.

396

### 397 **3.2 Budget Closure of ASOA for 4 Urban Areas on 3 Continents Indicates Reasonable** 398 **Understanding of ASOA Sources**

399 To investigate the correlation between ASOA and  $R_{\text{BTEX}}$ , a box model using the emission  
400 ratios from BTEX (Table S5), other aromatics (Table S8), IVOCs (Sect. S1), and SVOCs (Sect.  
401 S1) was run for five urban areas: New York City, 2002, Los Angeles, Beijing, London, and New  
402 York City, 2015 (see Sect. S1 and S3 for more information). The differences in the results shown  
403 in Fig. 4 are due to differences in the emissions for each city. We show that BTEX alone cannot  
404 explain the observed ASOA budget for urban areas around the world. Fig. 4a shows that  
405 approximately  $25\pm 6\%$  of the observed ASOA originates from the photooxidation of BTEX.  
406 BTEX only explaining 25% of the observed ASOA is similar to prior studies that have done  
407 budget analysis of precursor gases and observed SOA (e.g., Dzepina et al., 2009; Ensberg et al.,  
408 2014; Hayes et al., 2015; Ma et al., 2017; Nault et al., 2018). Therefore, other precursors must  
409 account for most of the ASOA produced.

410 Because alkanes, alkenes, and oxygenated compounds with carbon numbers less than 6  
411 are not significant ASOA precursors, we focus on emissions and sources of BTEX, other  
412 mono-aromatics, IVOCs, and SVOCs. These three classes of VOCs, aromatics, IVOCs, and  
413 SVOCs, have been suggested to be significant ASOA precursors in urban atmospheres  
414 (Robinson et al., 2007; Hayes et al., 2015; Ma et al., 2017; McDonald et al., 2018; Nault et al.,  
415 2018; Schroder et al., 2018; Shah et al., 2018), originating from both fossil fuel and VCP  
416 emissions.

417 Using the best available emission inventories from cities on three continents  
418 (EMEP/EEA, 2016; McDonald et al., 2018; Li et al., 2019) and observations, we quantify the  
419 emissions of BTEX, other mono-aromatics, IVOCs, and SVOCs for both fossil fuel (e.g.,  
420 gasoline, diesel, kerosene, etc.), VCPs (e.g., coatings, inks, adhesives, personal care products,  
421 and cleaning agents), and cooking sources (Fig. 5). This builds off the work of McDonald et al.  
422 (2018) for urban regions on three different continents.

423 Note, the emissions investigated here ignore any oxygenated VOC emissions not  
424 associated with IVOCs and SVOCs due to the challenge in estimating the emission ratios for  
425 these compounds (de Gouw et al., 2018). Further, SVOC emission ratios are estimated from the  
426 average POA observed by the AMS during the specific campaign and scaled by profiles in  
427 literature for a given average temperature and average OA (Robinson et al., 2007; Worton et al.,  
428 2014; Lu et al., 2018). As most of the campaigns had an average OA between 1 and 10  $\mu\text{g m}^{-3}$   
429 and temperature of  $\sim 298$  K, this led to the majority of the estimated emitted SVOC gases in the  
430 highest SVOC bin. However, as discussed later, this does not lead to SVOCs dominating the  
431 predicted ASOA due to taking into account the fragmentation and overall yield from the  
432 photooxidation of SVOC to ASOA.

433 Combining these inventories and observations for the various locations provide the  
434 following insights about the potential ASOA precursors not easily measured or quantified in  
435 urban environments (e.g., Zhao et al., 2014; Lu et al., 2018): (1) aromatics from fossil fuel  
436 accounts for 14-40% (mean 22%) of the total BTEX and IVOC emissions for the five urban  
437 areas investigated in-depth (Fig. 5), agreeing with prior studies that have shown that the observed  
438 ASOA cannot be reconciled by the observations or emission inventory of aromatics from fossil

439 fuels (e.g., Ensberg et al., 2014; Hayes et al., 2015). (2) BTEX from both fossil fuels and VCPs  
440 account for 25-95% (mean 43%) of BTEX and IVOC emissions (Fig. 5). China has the lowest  
441 contribution of IVOCs, potentially due to differences in chemical make-up of the solvents used  
442 daily (Li et al., 2019), but more research is needed to investigate the differences in IVOCs:BTEX  
443 from Beijing versus US and UK emission inventories. Nonetheless, this shows the importance of  
444 IVOCs for both emissions and ASOA precursors. (3) IVOCs are generally equal to, if not greater  
445 than, the emissions of BTEX in 4 of the 5 urban areas investigated here (Fig. 5). (4) Overall,  
446 VCPs account for a large fraction of the BTEX and IVOC emissions for all five cities. (5)  
447 Finally, SVOCs account for 27-88% (mean 53%) of VOCs generally considered ASOA  
448 precursors (VOCs with volatility saturation concentrations  $\leq 10^7 \mu\text{g m}^{-3}$ ) (Fig. S6). Beijing has  
449 the highest contribution of SVOCs to ASOA precursors due to the use of solid fuels and cooking  
450 emissions (Hu et al., 2016). Also, this indicates the large contribution of a class of VOCs  
451 difficult to measure (Robinson et al., 2007) that are an important ASOA precursor (e.g., Hayes et  
452 al., 2015), showing further emphasis should be placed in quantifying the emissions of this class  
453 of compounds.

454         These results provide an ability to further investigate the mass balance of predicted and  
455 observed ASOA for these urban locations (Fig. 4). The inclusion of IVOCs, other aromatics not  
456 including BTEX, and SVOCs leads to the ability to explain, on average,  $85\pm 12\%$  of the observed  
457 ASOA for these urban locations around the world (Fig. 4a). Further, VCP contribution to ASOA  
458 is important for all these urban locations, accounting for, on average,  $37\pm 3\%$  of the observed  
459 ASOA (Fig. 4b).

460 This bottom-up mass budget analysis provides important insights to further explain the  
461 correlation observed in Fig. 2. First, IVOCs are generally co-emitted from similar sources as  
462 BTEX for the urban areas investigated in-depth (Fig. 5). The oxidation of these co-emitted  
463 species leads to the ASOA production observed across the urban areas around the world. Second,  
464 S/IVOCs generally have similar rate constants as toluene and xylenes ( $\geq 1 \times 10^{-11} \text{ cm}^3 \text{ molec.}^{-1} \text{ s}^{-1}$ )  
465 (Zhao et al., 2014, 2017), the compounds that contribute the most to  $R_{\text{BTEX}}$ , explaining the rapid  
466 ASOA production that has been observed in various studies (de Gouw and Jimenez, 2009;  
467 DeCarlo et al., 2010; Hayes et al., 2013; Hu et al., 2013, 2016; Nault et al., 2018; Schroder et al.,  
468 2018) and correlation (Fig. 2). Finally, the contribution of VCPs and fossil fuel sources to ASOA  
469 is similar across the cities, expanding upon and further supporting the conclusion of McDonald  
470 et al. (2018) in the importance of identifying and understanding VCP emissions in order to  
471 explain ASOA.

472 This investigation shows that the bottom-up calculated ASOA agrees with observed  
473 top-down ASOA within 15%. As highlighted above, this ratio is explained by the co-emissions  
474 of IVOCs with BTEX from traditional sources (diesel, gasoline, and other fossil fuel emissions)  
475 and VCPs (Fig. 5) along with similar rate constants for these ASOA precursors (Table S12).  
476 Thus, the  $\text{ASOA}/R_{\text{BTEX}}$  ratio obtained from Fig. 2 results in accurate predictions of ASOA for the  
477 urban areas evaluated here, and this value can be used to better estimate ASOA with chemical  
478 transport models (Sect. 4).

479

#### 480 **4. Improved Urban SIMPLE Model Using Multi-Cities to Constrain**

481 The SIMPLE model was originally designed and tested against the observations collected  
482 around Mexico City (Hodzic and Jimenez, 2011). It was then tested against observations  
483 collected in Los Angeles (Hayes et al., 2015; Ma et al., 2017). As both data sets have nearly  
484 identical  $\Delta\text{SOA}/\Delta\text{CO}$  and  $R_{\text{BTEX}}$  (Fig. 2 and Fig. 3), it is not surprising that the SIMPLE model  
485 did well in predicting the observed  $\Delta\text{SOA}/\Delta\text{CO}$  for these two urban regions with consistent  
486 parameters. Though the SIMPLE model generally performed better than more explicit models, it  
487 generally had lower skill in predicting the observed ASOA in urban regions outside of Mexico  
488 City and Los Angeles (Shah et al., 2019; Pai et al., 2020).

489 This may stem from the original SIMPLE model with constant parameters missing the  
490 ability to change the amount and reactivity of the emissions, which are different for the various  
491 urban regions, versus the ASOA precursors being emitted proportionally to only CO (Hodzic and  
492 Jimenez, 2011; Hayes et al., 2015). For example, in the HTAP emissions inventory, the CO  
493 emissions for Seoul, Los Angeles, and Mexico City are all similar (Fig. S8); thus, the original  
494 SIMPLE model would suggest similar  $\Delta\text{SOA}/\Delta\text{CO}$  for all three urban locations. However, as  
495 shown in Fig. 2 and Fig. 3, the  $\Delta\text{SOA}/\Delta\text{CO}$  is different by nearly a factor of 2. The inclusion of  
496 the emissions and reactivity, where  $R_{\text{BTEX}}$  for Seoul is approximately a factor of 2.5 higher than  
497 Los Angeles and Seoul, into the improved SIMPLE model better accounts for the variability in  
498 SOA production, as shown in Fig. 2. Thus, the inclusion and use of this improved SIMPLE  
499 model refines the simplified representation of ASOA in chemical transport models and/or box  
500 models.

501 The “improved” SIMPLE shows higher ASOA compared to the default VBS  
502 GEOS-Chem (Fig. 6a,b). In areas strongly impacted by urban emissions (e.g., Europe, East Asia,

503 India, east and west coast US, and regions impacted by Santiago, Chile, Buenos Aires,  
504 Argentina, Sao Paulo, Brazil, Durban and Cape Town, South Africa, and Melbourne and Sydney,  
505 Australia), the “improved” SIMPLE model predicts up to  $14 \mu\text{g m}^{-3}$  more ASOA, or ~30 to 60  
506 times more ASOA than the default scheme (Fig. 6c,d). As shown in Fig. 1, during intensive  
507 measurements, the ASOA composed 17-39% of  $\text{PM}_{10}$ , with an average contribution of ~25%. The  
508 default ASOA scheme in GEOS-Chem greatly underestimates the fractional contribution of  
509 ASOA to total  $\text{PM}_{2.5}$  (<2%; Fig. 6e). The “improved” SIMPLE model greatly improves the  
510 predicted fractional contribution, showing that ASOA in the urban regions ranges from 15-30%,  
511 with an average of ~15% for the grid cells corresponding to the urban areas investigated here  
512 (Fig. 6f). Thus, the “improved” SIMPLE predicts the fractional contribution of ASOA to total  
513  $\text{PM}_{2.5}$  far more realistically, compared to observations. As discussed in Sect. 2.3 and Eq. 11,  
514 having the model accurately predict the fractional contribution of ASOA to the total PM is very  
515 important, as the total  $\text{PM}_{2.5}$  is derived from satellite-based estimates (van Donkelaar et al.,  
516 2015), and the model fractions are then applied to those total  $\text{PM}_{2.5}$  estimates. The ability for the  
517 “improved” SIMPLE model to better represent the ASOA composition provides confidence  
518 attributing the ASOA contribution to premature mortality.

519

## 520 **5. Preliminary Evaluation of Worldwide Premature Deaths Due to ASOA with Updated** 521 **SIMPLE Parameterization**

522 The improved SIMPLE parameterization is used along with GEOS-Chem to provide an  
523 accurate estimation of ASOA formation in urban areas worldwide and provide an ability to  
524 obtain realistic simulations of ASOA based on measurement data. We use this model to quantify



525 the attribution of  $PM_{2.5}$  ASOA to premature deaths. Analysis up to this point has been for  $PM_1$ ;  
526 however, both the chemical transport model and epidemiological studies utilize  $PM_{2.5}$ . For  
527 ASOA, this will not impact the discussion and results here because the mass of OA (typically  
528 80–90%) is dominated by  $PM_1$  (e.g., Bae et al., 2006; Seinfeld and Pandis, 2006), and ASOA is  
529 formed mostly through condensation of oxidized species, which favors partitioning onto smaller  
530 particles (Seinfeld and Pandis, 2006).

531 The procedure for this analysis is described in Fig. 7 and Sect. 2.3 and S3. Briefly, we  
532 combine high-resolution satellite-based  $PM_{2.5}$  estimates (for exposure) and a chemical transport  
533 model (GEOS-Chem, for fractional composition) to estimate ASOA concentrations and various  
534 sensitivity analysis (van Donkelaar et al., 2015). We calculated ~3.3 million premature deaths  
535 (using the Integrated Exposure-Response, IER, function) are due to long-term exposure of  
536 ambient  $PM_{2.5}$  (Fig. S9, Table S16), consistent with recent literature (Cohen et al., 2017).

537 The attribution of ASOA  $PM_{2.5}$  premature deaths can be calculated one of two ways: (a)  
538 marginal method (Silva et al., 2016) or (b) attributable fraction method (Anenberg et al., 2019).  
539 For method (a), it is assumed that a fraction of the ASOA is removed, keeping the rest of the  
540  $PM_{2.5}$  components approximately constant, and the change in deaths is calculated from the deaths  
541 associated with the total concentration less the deaths calculated using the reduced total  $PM_{2.5}$   
542 concentrations. For method (b), the health impact is attributed to each  $PM_{2.5}$  component by  
543 multiplying the total deaths by the fractional contribution of each component to total  $PM_{2.5}$ . For  
544 method (a), the deaths attributed to ASOA are ~340,000 people per year (Fig. 8); whereas, for  
545 method (b), the deaths are ~370,000 people per year. Both of these are based on the IER response  
546 function (Cohen et al., 2017).

547 Additional recent work (Burnett et al., 2018) has suggested less reduction in the  
548 premature deaths versus  $PM_{2.5}$  concentration relationship at higher  $PM_{2.5}$  concentrations, and  
549 lower concentration limits for the threshold below which this relationship is negligible, both of  
550 which lead to much higher estimates of  $PM_{2.5}$  associated premature deaths. This is generally  
551 termed the Global Exposure Mortality Model (GEMM). Using the two attribution methods  
552 described above (a and b), the ASOA  $PM_{2.5}$  premature deaths are estimated to be ~640,000  
553 (method a) and ~900,000 (method b) (Fig. S9 and Fig. S12 and Table S17).

554 Compared to prior studies using chemical transport models to estimate premature deaths  
555 associated with ASOA (e.g., Silva et al., 2016; Ridley et al., 2018), which assumed non-volatile  
556 POA and “traditional” ASOA precursors, the attribution of premature mortality due to ASOA is  
557 over an order of magnitude higher in this study (Fig. 9). This occurs using either the IER and  
558 GEMM approach for estimating premature mortality (Fig. 9). For regions with larger populations  
559 and more  $PM_{2.5}$  pollution, the attribution is between a factor of 40 to 80 higher. This stems from  
560 the non-volatile POA and “traditional” ASOA precursors over-estimating POA and  
561 under-estimating ASOA compared to observations (Schroder et al., 2018). These offsetting  
562 errors will lead to model predicted total OA similar to observations (Ridley et al., 2018; Schroder  
563 et al., 2018), yet different conclusions on whether POA versus SOA is more important for  
564 reducing  $PM_{2.5}$  associated premature mortality. Using a model constrained to day-time  
565 atmospheric observations (Fig. 2 and Fig. 4, see Sect. 4) leads to a more accurate estimation of  
566 the contribution of photochemically-produced ASOA to  $PM_{2.5}$  associated premature mortality  
567 that has not been possible in prior studies. We note that ozone concentrations change little as we  
568 change the ASOA simulation (see Sect. S4 and Fig. S14).

569 A limitation in this study is the lack of sufficient measurements in South and Southeast  
570 Asia, Eastern Europe, Africa, and South America (Fig. 1), though these areas account for 44% of  
571 the predicted reduction in premature mortality for the world (Table S16). However, as  
572 highlighted in Table S18, these regions likely still consume both transportation fuels and VCPs,  
573 although in lower per capita amounts than more industrialized countries. This consumption is  
574 expected to lead to the same types of emissions as for the cities studied here, though more field  
575 measurements are needed to validate global inventories of VOCs and resulting oxidation  
576 products in the developing world. Transportation emissions of VOCs are expected to be more  
577 dominant in the developing world due to higher VOC emission factors associated with inefficient  
578 combustion engines, such as two-stroke scooters (Platt et al., 2014) and auto-rickshaws (e.g.,  
579 Goel and Guttikunda, 2015).

580 Solid fuels are used for residential heating and cooking, which impact the outdoor air  
581 quality as well (Hu et al., 2013, 2016; Lacey et al., 2017; Stewart et al., 2020), and which also  
582 lead to SOA (Heringa et al., 2011). As discussed in Sect. 3.1, though the majority of the studies  
583 evaluated here occurred in spring to summer time, when solid fuel emissions are decreased, two  
584 studies occurred during the winter/early spring time, where solid fuel emissions were important  
585 (Hu et al., 2013; Schroder et al., 2018). These studies still follow the same relationship between  
586 ASOA and  $R_{\text{BTEX}}$  as the studies that focused on spring/summer time photochemistry. Thus, the  
587 limited datasets available indicate that photochemically produced ASOA from solid fuels follow  
588 a similar relationship to that from other ASOA sources.

589 Also, solid fuel sources are included in the inventories used in our modeling. For the  
590 HTAP emission inventory used here (Janssens-Maenhout et al., 2015), small-scale combustion,

591 which includes heating and cooking (e.g., solid-fuel use), is included in the residential emission  
592 sector. Both CO and BTEX are included in this source, and can account for a large fraction of the  
593 total emissions where solid-fuel use may be important (Fig. S15). Thus, as CO and BTEX are  
594 used in the updated SIMPLE model, and campaigns that observed solid-fuel emissions fall  
595 within the trend for all urban areas, the solid-fuel contribution to photochemically-produced  
596 ASOA is accounted for (as accurately as allowed by current datasets) in the estimation of ASOA  
597 for the attribution to premature mortality.

598         Note that recent work has observed potential nighttime aqueous chemistry and/or  
599 oxidation by nitrate radical from solid fuel emissions to produce ASOA (Kodros et al., 2020).  
600 Thus, missing this source of ASOA may lead to an underestimation of total ASOA versus the  
601 photochemically-produced ASOA we discuss here, leading to a potential underestimation in the  
602 attribution of ASOA to premature mortality. From the studies that investigated “night-time  
603 aging” of solid-fuel emissions to form SOA, we predict that the total ASOA may be  
604 underestimated by 1 to 3  $\mu\text{g m}^{-3}$  (Kodros et al., 2020). This potential underestimation, though, is  
605 less than the current underestimation in ASOA in GEOS-Chem (default versus “Updated”  
606 SIMPLE).

607         Recently, emission factors from Abidjan, Côte d’Ivoire, a developing urban area, showed  
608 the dominance of emissions from transportation and solid fuel burning, with BTEX being an  
609 important fraction of the total emissions, and that all the emissions were efficient in producing  
610 ASOA (Dominutti et al., 2019). Further, investigation of emissions in New Delhi region of India  
611 demonstrated the importance of both transportation and solid fuel emissions (Stewart et al.,  
612 2020; Wang et al., 2020) while model comparisons with observations show an underestimation

613 of OA compared to observations due to a combination of emissions and OA representation (Jena  
614 et al., 2020). Despite emission source differences, SOA is still an important component of  $PM_{2.5}$   
615 (e.g., Singh et al., 2019) and thus will impact air quality and premature mortality in developing  
616 regions. Admittedly, though, our estimates will be less accurate for these regions.

617

## 618 **6. Conclusions**

619 In summary, ASOA is an important, though inadequately constrained component of air  
620 pollution in megacities and urban areas around the world. This stems from the complexity  
621 associated with the numerous precursor emission sources, chemical reactions, and oxidation  
622 products that lead to observed ASOA concentrations. We have shown here that the variability in  
623 observed ASOA across urban areas is correlated with  $R_{\text{BTEX}}$ , a marker for the co-emissions of  
624 IVOC from both transportation and VCP emissions. Global simulations indicate ASOA  
625 contributes to a substantial fraction of the premature mortality associated with  $PM_{2.5}$ . Reductions  
626 of the ASOA precursors will reduce the premature deaths associated with  $PM_{2.5}$ , indicating the  
627 importance of identifying and reducing exposure to sources of ASOA. These sources include  
628 emissions that are both traditional (transportation) as well as non-traditional emissions of  
629 emerging importance (VCPs) to ambient  $PM_{2.5}$  concentrations in cities around the world. Further  
630 investigation of speciated IVOCs and SVOCs for urban areas around the world along with SOA  
631 mass concentration and other photochemical products (e.g.,  $O_x$ , PAN, and HCHO) for other  
632 urban areas, especially in South Asia, throughout Africa, and throughout South America, would  
633 provide further constraints to improve the SIMPLE model and our understanding of the emission  
634 sources and chemistry that leads to the observed SOA and its impact on premature mortality.

## 635 Acknowledgements

636

637 This study was partially supported by grants from NASA NNX15AT96G, NNX16AQ26G, Sloan  
638 Foundation 2016-7173, NSF AGS-1822664, EPA STAR 83587701-0, NERC NE/H003510/1,  
639 NERC NE/H003177/1, NERC NE/H003223/1, NOAA NA17OAR4320101, NCAS  
640 R8/H12/83/037, Natural Science and Engineering Research Council of Canada (NSERC,  
641 RGPIN/05002-2014), and the Fonds de Recherche du Québec —Nature et technologies  
642 (FRQNT, 2016-PR-192364). This manuscript has not been formally reviewed by EPA. The  
643 views expressed in this document are solely those of the authors and do not necessarily reflect  
644 those of the Agency. EPA does not endorse any products or commercial services mentioned in  
645 this publication. We thank Katherine Travis for useful discussions. We acknowledge B J. Bandy,  
646 J. Lee, G. P. Mills, d. D. Montzka, J. Stutz, A. J. Weinheimer E. J. Williams, E. C. Wood, and D.  
647 R. Worsnop for use of their data.

648

## 649 Data Availability

650 TexAQS measurements are available at  
651 <https://esrl.noaa.gov/csl/groups/csl7/measurements/2000TexAQS/LaPorte/DataDownload/> and  
652 upon request. NEAQS measurements are available at  
653 <https://www.esrl.noaa.gov/csl/groups/csl7/measurements/2002NEAQS/>. MILAGRO  
654 measurements are available at <http://doi.org/10.5067/Aircraft/INTEXB/Aerosol-TraceGas>.  
655 CalNex measurements are available at  
656 <https://esrl.noaa.gov/csl/groups/csl7/measurements/2010calnex/Ground/DataDownload/>.  
657 ClearfLo measurements are available at  
658 <https://catalogue.ceda.ac.uk/uuid/6a5f9eedd68f43348692b3bace3eba45>. SEAC<sup>4</sup>RS measurements  
659 are available at <http://doi.org/10.5067/Aircraft/SEAC4RS/Aerosol-TraceGas-Cloud>. WINTER  
660 measurements are available at [https://data.eol.ucar.edu/master\\_lists/generated/winter/](https://data.eol.ucar.edu/master_lists/generated/winter/).  
661 KORUS-AQ measurements are available at  
662 <http://doi.org/10.5067/Suborbital/KORUSAQ/DATA01>. Data from Chinese campaigns are  
663 available upon request, and rest of data used were located in papers cited. GEOS-Chem data  
664 available upon request. Figures will become accessible at  
665 [cires1.colorado.edu/jimenez/group\\_pubs.html](https://cires1.colorado.edu/jimenez/group_pubs.html).

666

## 667 Competing Interests

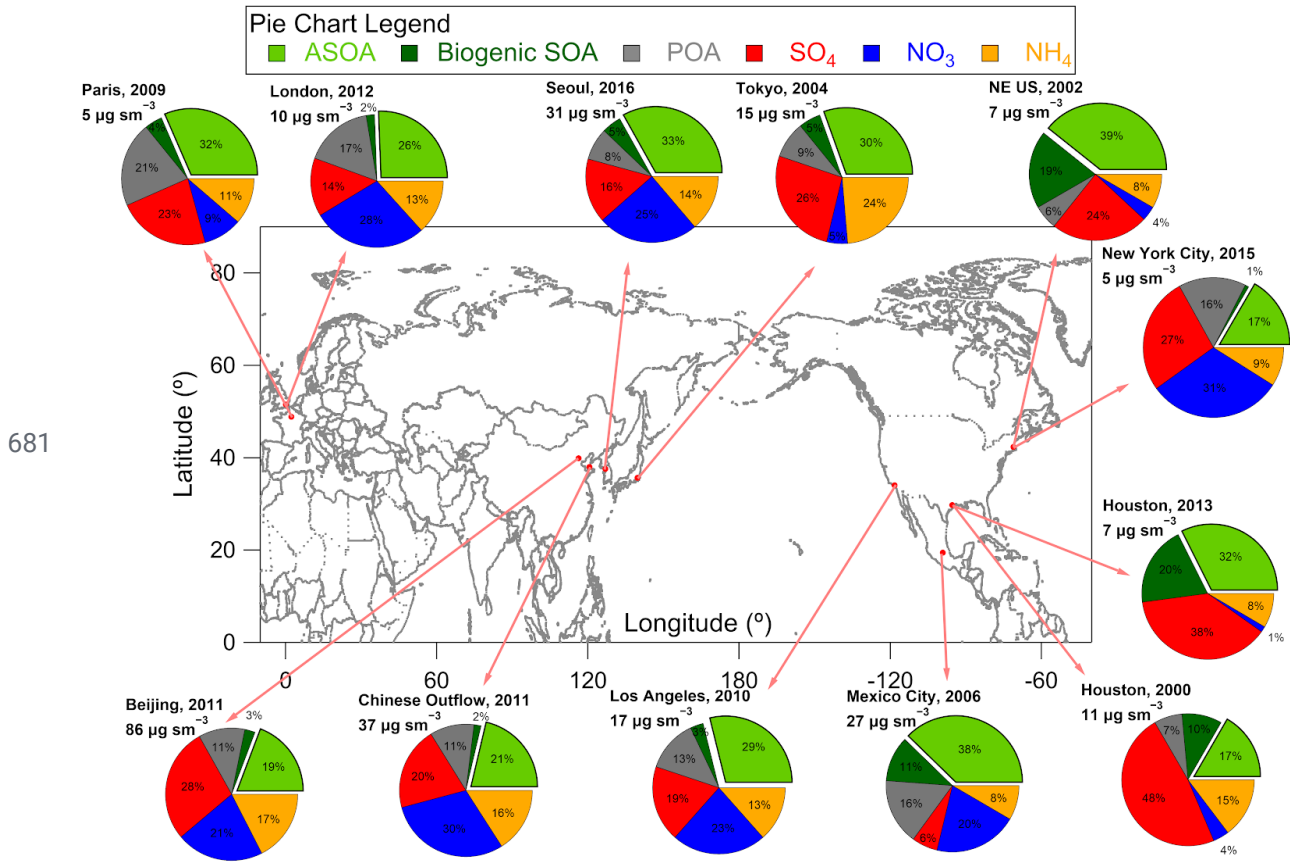
668 The authors declare no competing interests.

669

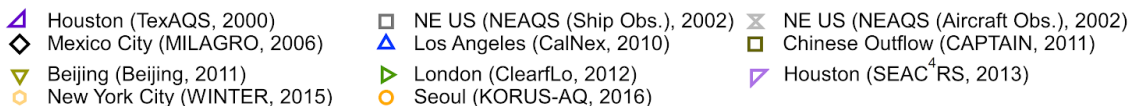
## 670 Author Contribution

671 B.A.N., D.S.J., B.C.M., J.A.dG., and J.L.J designed the experiment and wrote the paper. B.A.N.,  
672 PC.-J., D.A.D., W.H., J.C.S, J.A., D.R.B., M.R.C., H.C., M.M.C., P.F.D, G.S.D., R.D., F.F, A.F.,  
673 J.B.G., G.G., J.F.H, T.F.H., P.L.H., J.H., M.H., L.G.H., B.T.J., W.C.K., J.L., I.B.P., J.P., B.R.,

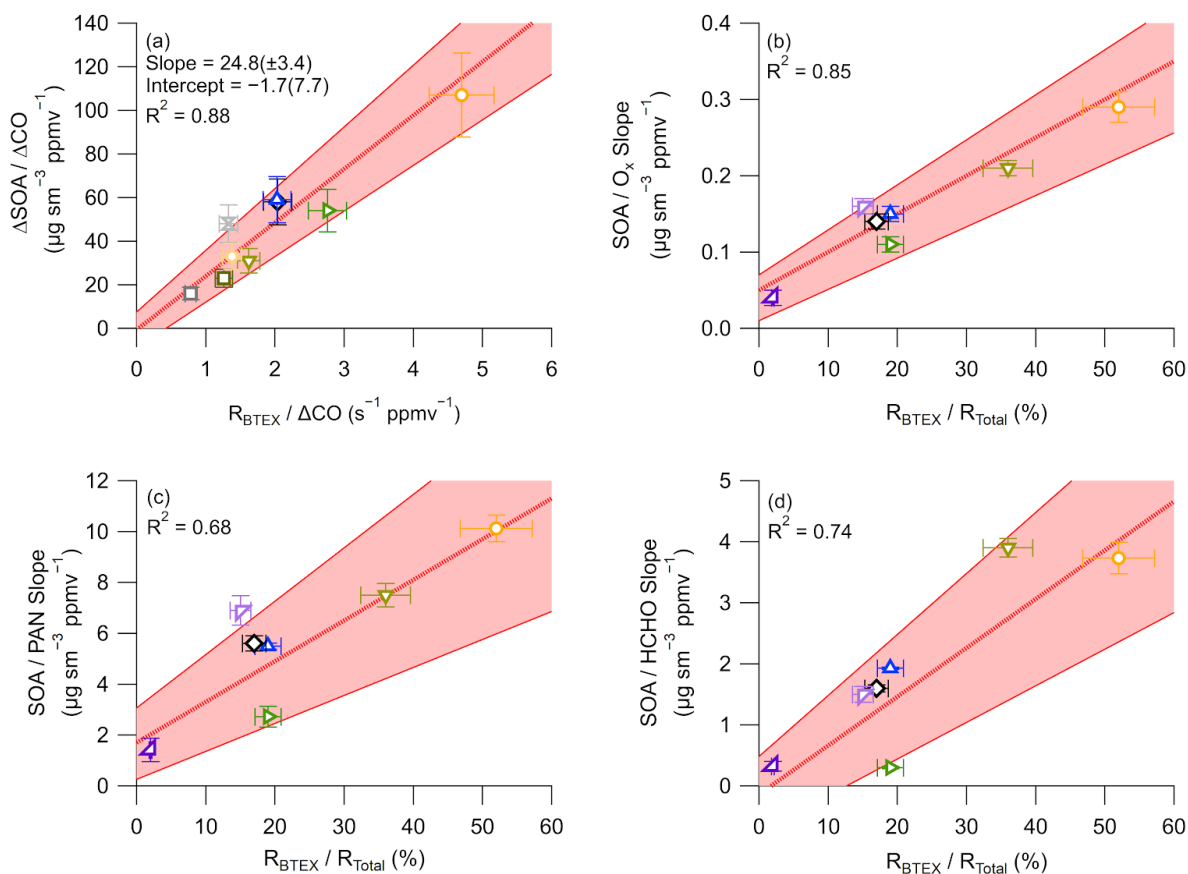
674 C.E.R., D.R., J.M.R., T.B.R, M.S., J.W., C.W., P.W., G.M.W., D.E.Y., B.Y., J.A.dG., and J.L.J.  
675 collected and analyzed the data. D.S.J. and A.H. ran the GEOS-Chem model and B.A.N., D.S.J,  
676 and J.L.J. analyzed the model output. B.A.N., P.L.H., J.M.S., and J.L.J. ran and analyzed the 0-D  
677 model used for ASOA budget analysis of ambient observations. B.C.M., A.L., M.L., and Q.Z.  
678 analyzed and provided the emission inventories used for the 0-D box model. D.S.J., D.K.H., and  
679 M.O.N. conducted the ASOA attribution to mortality calculation, and B.A.N., D.S.J., D.K.H.,  
680 M.O.N., J.A.dG, and J.L.J analyzed the results. All authors reviewed the paper.





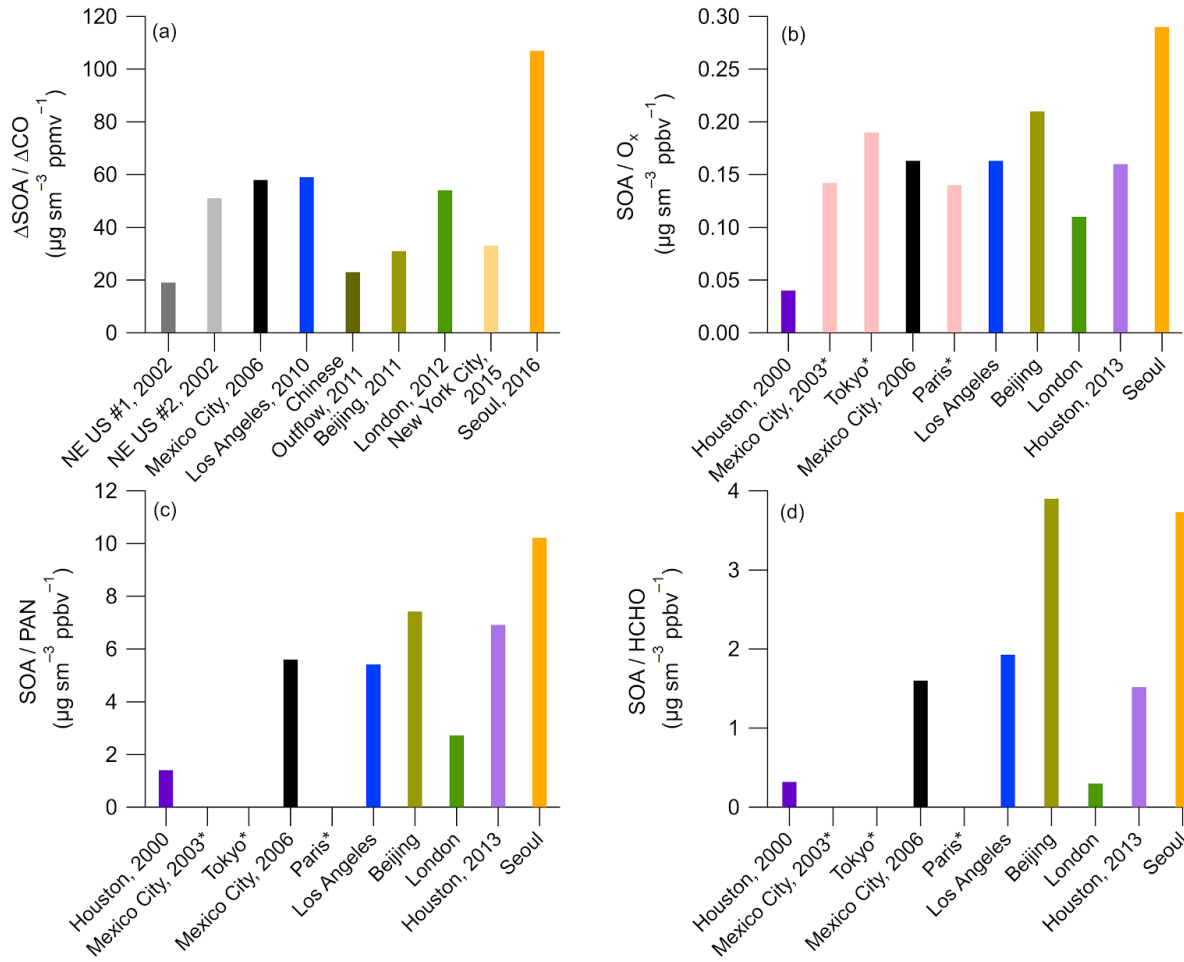


686



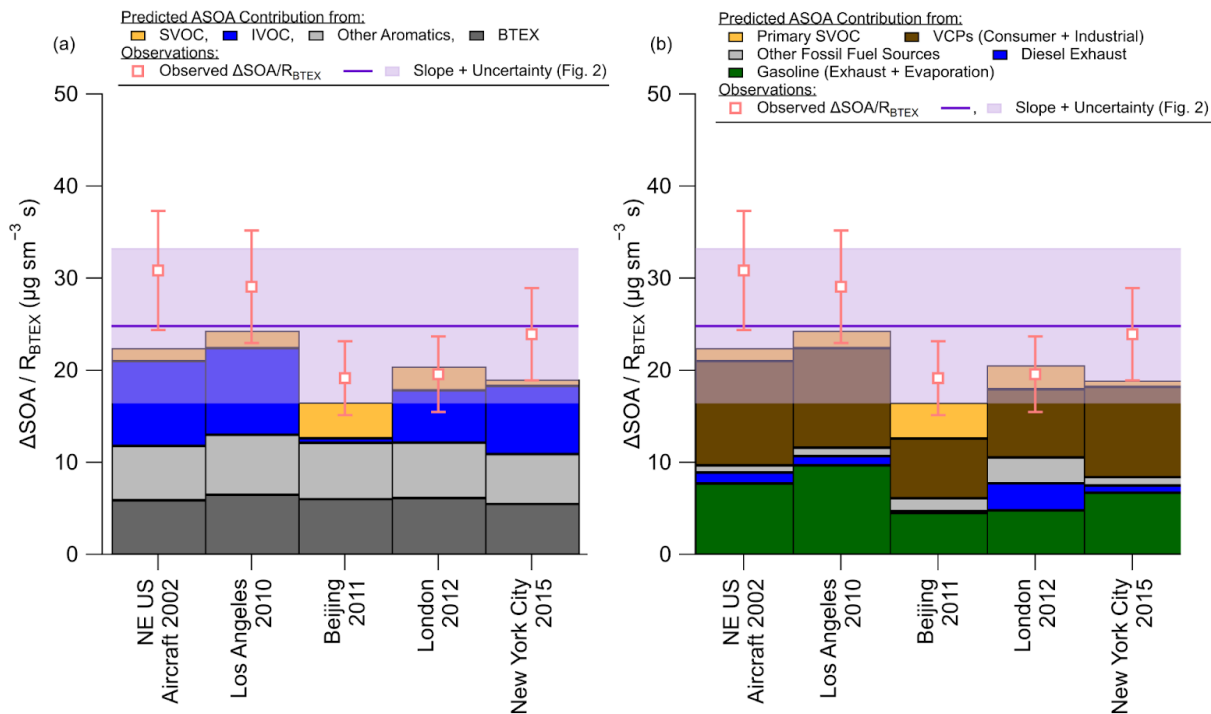
687 **Figure 2.** (a) Scatter plot of background and dilution corrected ASOA concentrations  
 688 ( $\Delta\text{SOA}/\Delta\text{CO}$  at PA = 0.5 equivalent days) versus BTEX emission reactivity ratio ( $R_{\text{BTEX}} =$   
 689  $\sum_i [\text{VOC}/\text{CO}]_i$ ) for multiple major field campaigns on three continents. Comparison of ASOA  
 690 versus (b) O<sub>x</sub>, (c) PAN, and (d) HCHO slopes versus the ratio of the BTEX/Total emission  
 691 reactivity, where total is the OH reactivity for the emissions of BTEX + C2-3 alkenes + C2-6  
 692 alkanes (Table S5 through Table S7), for the campaigns studied here. For all figures, red shading  
 693 is the  $\pm 1\sigma$  uncertainty of the slope, and the bars are  $\pm 1\sigma$  uncertainty of the data (see Sect. S5).

694

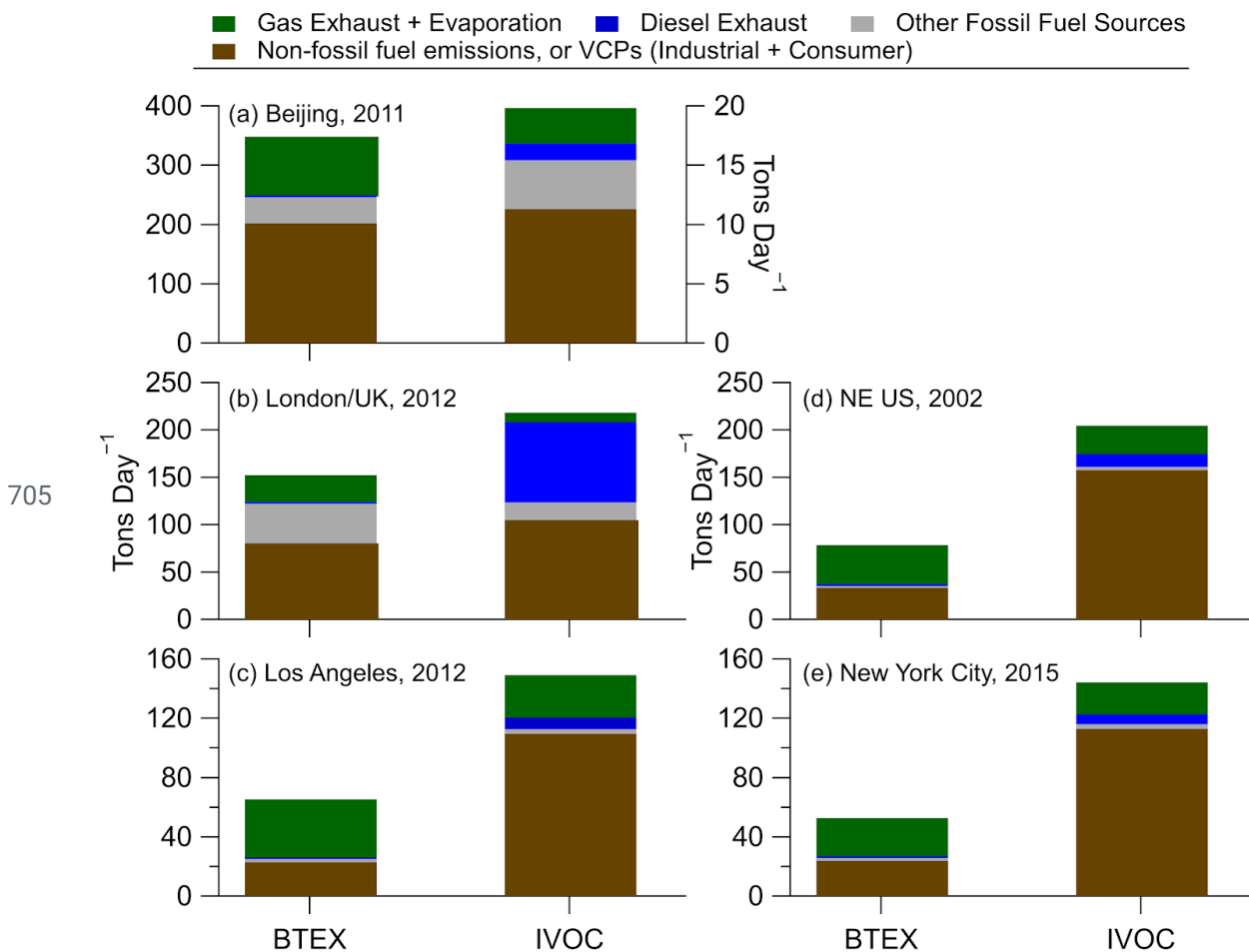


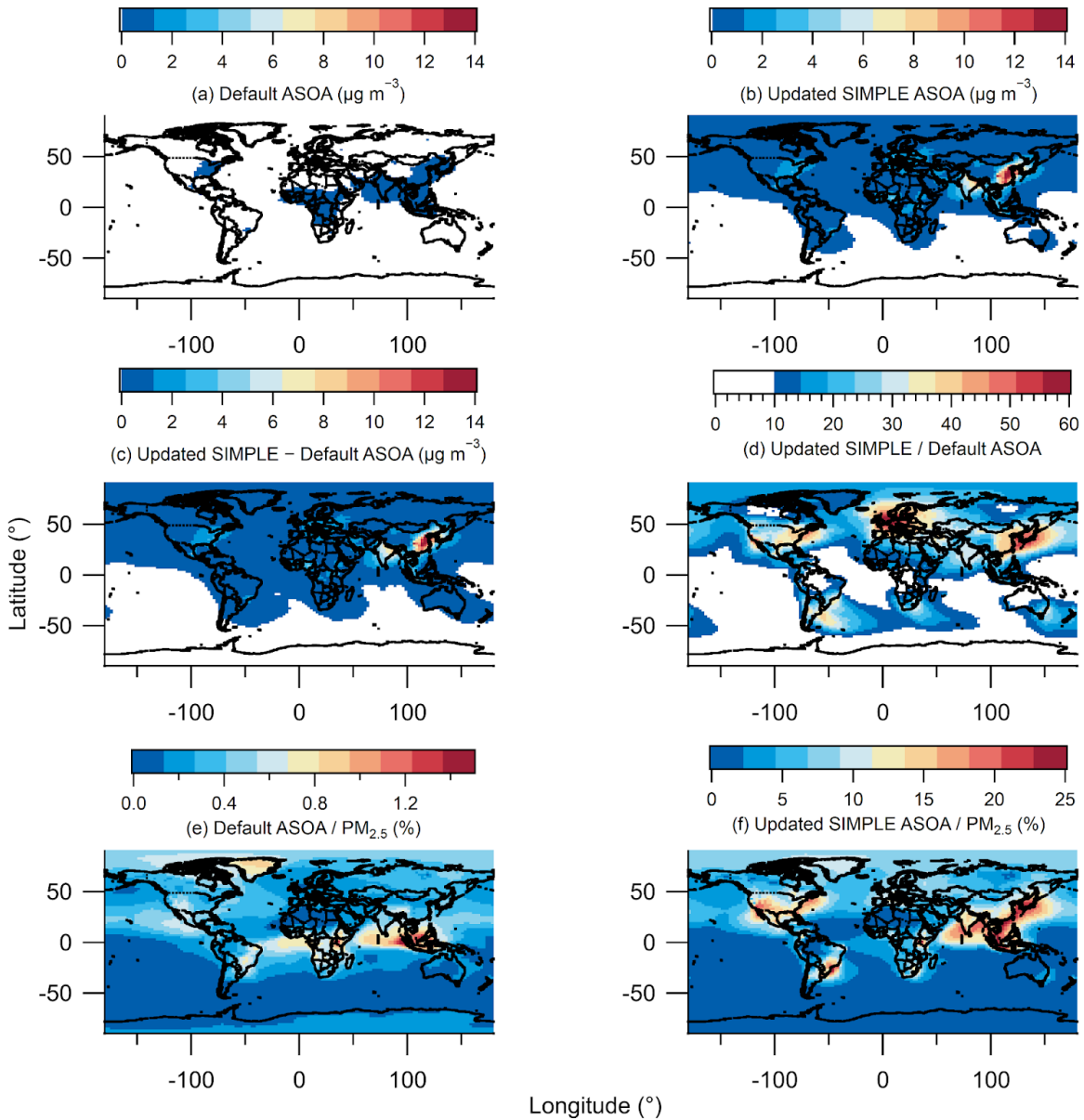
695 **Figure 3.** (a) A comparison of the  $\Delta\text{SOA}/\Delta\text{CO}$  for the urban campaigns on three continents.  
 696 Comparison of (b)  $\text{SOA}/\text{O}_x$ , (c)  $\text{SOA}/\text{HCHO}$ , and (d)  $\text{SOA}/\text{PAN}$  slopes for the urban areas  
 697 (Table S4). For (b) through (d), cities marked with \* have no HCHO, PAN, or hydrocarbon data.

698

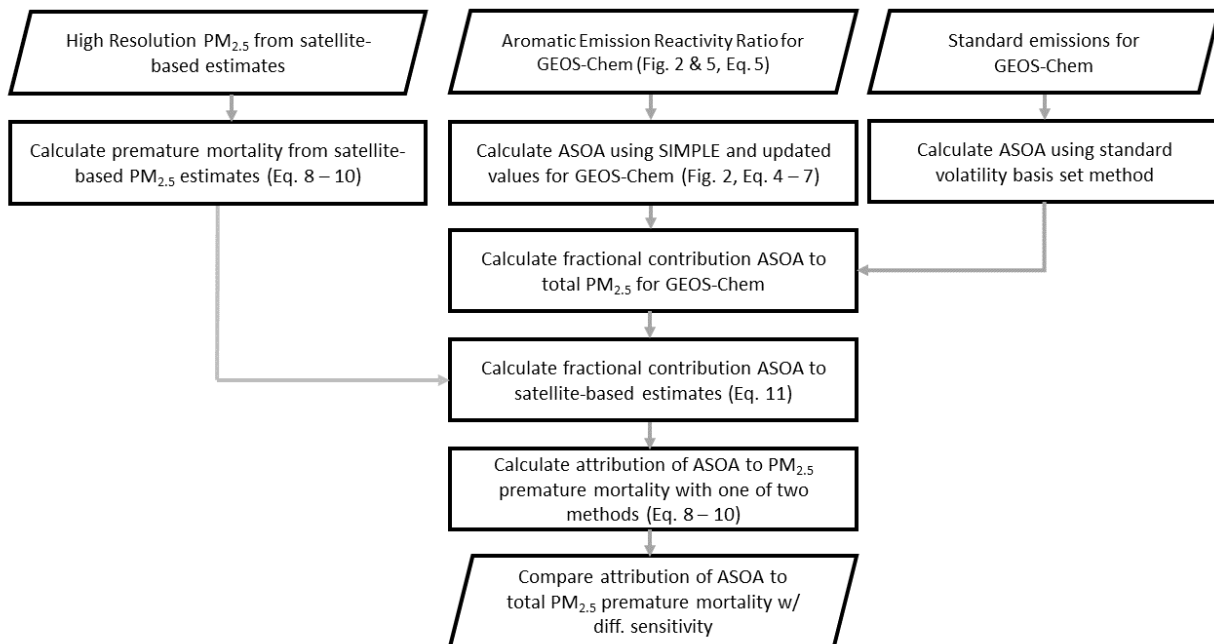


699 **Figure 4.** (a) Budget analysis for the contribution of the observed  $\Delta\text{SOA}/R_{\text{BTEX}}$  (Fig. 2) for cities  
 700 with known emissions inventories for different volatility classes (see SI and Fig. 5 and Fig. S6).  
 701 (b) Same as (a), but for sources of emissions. For (a) and (b), SVOC is the contribution from  
 702 both vehicle and other (cooking, etc.) sources. See SI for information about the emissions,  
 703 ASOA precursor contribution, error analysis, and discussion about sensitivity of emission  
 704 inventory IVOC/BTEX ratios for different cities and years in the US.



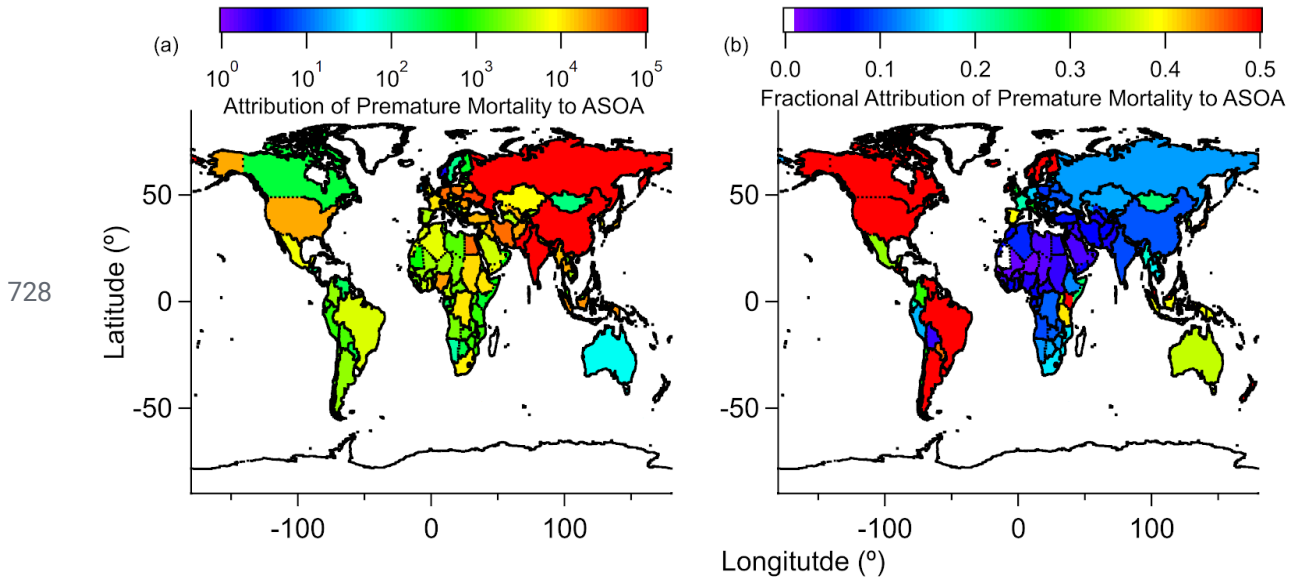


712 **Figure 6.** (a) Annual average modeled ASOA using the default VBS. (b) Annual average  
 713 modeled ASOA using the updated SIMPLE model. (c) Difference between annual average  
 714 modeled updated SIMPLE and default VBS. (d) Ratio between annual average modeled updated  
 715 SIMPLE and default VBS. (e) Percent contribution of annual average modeled ASOA using  
 716 default VBS to total modelled PM<sub>2.5</sub>. (f) Percent contribution of annual average modeled ASOA  
 717 using updated SIMPLE to total modelled PM<sub>2.5</sub>.

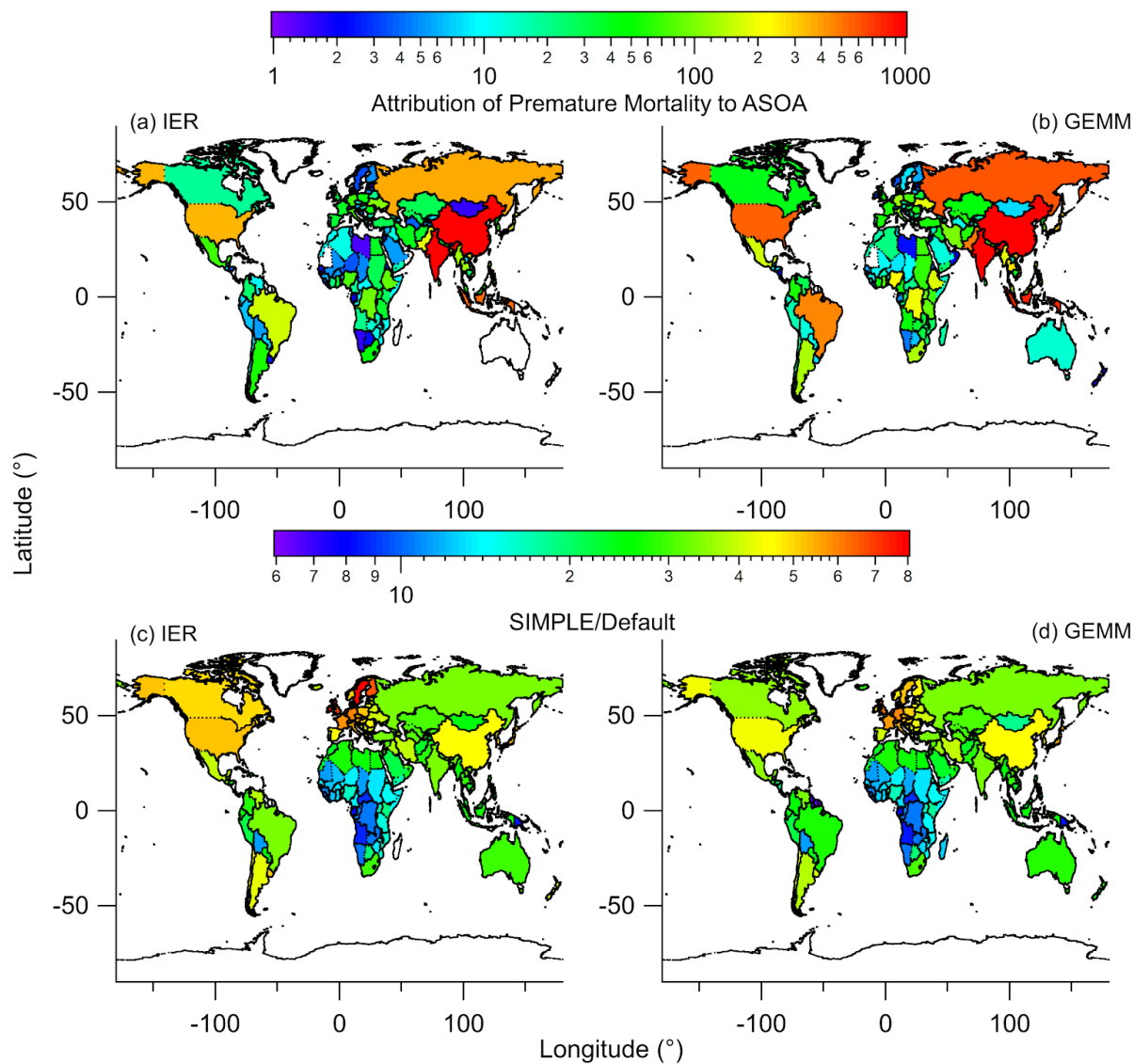


718

719 **Figure 7.** Flowchart describing how observed ASOA production was used to calculate ASOA in  
 720 GEOS-Chem, and how the satellite-based PM<sub>2.5</sub> estimates and GEOS-Chem PM<sub>2.5</sub> speciation was  
 721 used to estimate the premature mortality and attribution of premature mortality by ASOA. See  
 722 Sect. 2 and SI for further information about the details in the figure. SIMPLE is described in  
 723 Eq. 4 and by Hodzic and Jimenez (2011) and Hayes et al. (2015). The one of two methods  
 724 mentioned include either the Integrated Exposure-Response (IER) (Burnett et al., 2014) with  
 725 Global Burden of Disease (GBD) dataset (IHME, 2016) or the new Global Exposure Mortality  
 726 Model (GEMM) (Burnett et al., 2018) methods. For both IER and GEMM, the marginal method  
 727 (Silva et al., 2016) or attributable fraction method (Anenberg et al., 2019) are used.



729 **Figure 8.** Five-year average (a) estimated reduction in  $PM_{2.5}$ -associated premature deaths, by  
 730 country, upon removing ASOA from total  $PM_{2.5}$ , and (b) fractional reduction (reduction  $PM_{2.5}$   
 731 premature deaths / total  $PM_{2.5}$  premature deaths) in  $PM_{2.5}$ -associated premature deaths, by  
 732 country, upon removing ASOA from GEOS-Chem. The IER methods are used here. See Fig. S9  
 733 and Fig. S12 for results using GEMM. See Fig. S10 for  $10 \times 10$  km<sup>2</sup> area results in comparison  
 734 with country-level results.



735

736 **Figure 9.** Attribution of premature mortality to ASOA using (a) IER or (b) GEMM, using the  
 737 non-volatile primary OA and traditional SOA precursor method in prior studies (e.g., Ridley et  
 738 al., 2018). The increase in attribution of premature mortality to ASOA for the “SIMPLE” model  
 739 (Fig. 8) versus the non-volatile primary OA and traditional SOA precursor method (“Default”),  
 740 for (c) IER and (d) GEMM.



741 **Table 1.** List of campaigns used here. For values previously reported for those campaigns, they  
 742 are noted. For Seasons, W = Winter, Sp = Spring, and Su = Summer.

Location	Field Campaign	Coordinates		Time Period	Season	Previous Publication/Campaign Overview
		Long. (°)	Lat. (°)			
Houston, TX, USA (2000)	TexAQS 2000	-95.4	29.8	15/Aug/2000 - 15/Sept/2000	Su	Jimenez et al. (2009) <sup>a</sup> , Wood et al. (2010) <sup>b</sup>
Northeast USA (2002)	NEAQS 2002	-78.1 - -70.5	32.8 - 43.1	26/July/2002; 29/July/2002 - 10/Aug/2002	Su	Jimenez et al. (2009) <sup>a</sup> , de Gouw and Jimenez (2009) <sup>c</sup> , Kleinman et al. (2007) <sup>c</sup>
Mexico City, Mexico (2003)	MCMA-2003	-99.2	19.5	31/Mar/2003 - 04/May/2003	Sp	Molina et al. (2007), Herndon et al. (2008) <sup>b</sup>
Tokyo, Japan (2004)		139.7	35.7	24/July/2004 - 14/Aug/2004	Su	Kondo et al. (2008) <sup>a</sup> , Miyakawa et al. (2008) <sup>a</sup> , Morino et al. (2014) <sup>b</sup>
Mexico City, Mexico (2006)	MILAGRO	-99.4 - -98.6	19.0 - 19.8	04/Mar/2006 - 29/Mar/2006	Sp	Molina et al. (2010), DeCarlo et al. (2008) <sup>a</sup> , Wood et al. (2010) <sup>b</sup> , DeCarlo et al. (2010) <sup>c</sup>
Paris, France (2009)	MEGAPOLI	48.9	2.4	13/July/2009 - 29/July/2009	Su	Frenay et al. (2014) <sup>a</sup> , Zhang et al. (2015) <sup>b</sup>
Pasadena, CA, USA (2010)	CalNex	-118.1	34.1	15/May/2010 - 16/June/2010	Sp	Ryerson et al. (2013), Hayes et al. (2013) <sup>a,b,c</sup>
Changdao Island, China (2011)	CAPTAIN	120.7	38.0	21/Mar/2011 - 24/Apr/2011	Sp	Hu et al. (2013) <sup>a,c</sup>
Beijing, China (2011)	CareBeijing 2011	116.4	39.9	03/Aug/2011 - 15/Sept/2011	Su	Hu et al. (2016) <sup>a,b,c</sup>
London, UK (2012)	ClearfLo	0.1	51.5	22/July/2012 - 18/Aug/2012	Su	Bohnenstengel et al. (2015)
Houston, TX, USA (2013)	SEAC <sup>4</sup> RS	-96.0 - -94.0	29.2 - 30.3	01/Aug/2013 - 23/Sept/2013	Su	Toon et al. (2016)
New York City, NY, USA (2015)	WINTER	-74.0 - -69.0	39.5 - 42.5	07/Feb/2015	W	Schroder et al. (2018) <sup>a,c</sup>
Seoul, South Korea (2016)	KORUS-AQ	124.6 - 128.0	36.8 - 37.6	01/May/2016 - 10/June/2016	Sp	Nault et al. (2018) <sup>a,b,c,d</sup>

743 <sup>a</sup>Reference used for PM<sub>1</sub> composition. <sup>b</sup>Reference used for SOA/O<sub>x</sub> slope. <sup>c</sup>Reference used for  
 744 ΔOA/ΔCO value. <sup>d</sup>Reference used for SOA/HCHO and SOA/PAN slopes

## 745 References

- 746 Anenberg, S., Miller, J., Henze, D. and Minjares, R.: A global snapshot of the air  
747 pollution-related health impacts of transportation sector emissions in 2010 and 2015, ICCT,  
748 Climate & Clean Air Coalition., 2019.
- 749 Atkinson, R. and Arey, J.: Atmospheric Degradation of Volatile Organic Compounds, *Chem.*  
750 *Rev.*, 103, 4605–4638, 2003.
- 751 Atkinson, R., Baulch, D. L., Cox, R. A., Crowley, J. N., Hampson, R. F., Hynes, R. G., Jenkin,  
752 M. E., Rossi, M. J., Troe, J. and IUPAC Subcommittee: Evaluated kinetic and photochemical  
753 data for atmospheric chemistry: Volume II - gas phase reactions of organic species, *Atmos.*  
754 *Chem. Phys.*, 6(11), 3625–4055, 2006.
- 755 Bae, M.-S., Demerjian, K. L. and Schwab, J. J.: Seasonal estimation of organic mass to organic  
756 carbon in PM<sub>2.5</sub> at rural and urban locations in New York state, *Atmos. Environ.*, 40(39),  
757 7467–7479, 2006.
- 758 Baker, K. R., Woody, M. C., Valin, L., Szykman, J., Yates, E. L., Iraci, L. T., Choi, H. D., Soja,  
759 A. J., Koplitz, S. N., Zhou, L., Campuzano-Jost, P., Jimenez, J. L. and Hair, J. W.: Photochemical  
760 model evaluation of 2013 California wild fire air quality impacts using surface, aircraft, and  
761 satellite data, *Sci. Total Environ.*, 637-638, 1137–1149, 2018.
- 762 Bertram, T. H., Perring, A. E., Wooldridge, P. J., Crouse, J. D., Kwan, A. J., Wennberg, P. O.,  
763 Scheuer, E., Dibb, J., Avery, M., Sachse, G., Vay, S. A., Crawford, J. H., McNaughton, C. S.,  
764 Clarke, A., Pickering, K. E., Fuelberg, H., Huey, G., Blake, D. R., Singh, H. B., Hall, S. R.,  
765 Shetter, R. E., Fried, A., Heikes, B. G. and Cohen, R. C.: Direct Measurements of the Convective  
766 Recycling of the Upper Troposphere, *Science*, 315(5813), 816–820, 2007.
- 767 Bohnenstengel, S. I., Belcher, S. E., Aiken, A., Allan, J. D., Allen, G., Bacak, A., Bannan, T. J.,  
768 Barlow, J. F., Beddows, D. C. S., Bloss, W. J., Booth, A. M., Chemel, C., Coceal, O., Di Marco,  
769 C. F., Dubey, M. K., Faloon, K. H., Fleming, Z. L., Furger, M., Gietl, J. K., Graves, R. R., Green,  
770 D. C., Grimmond, C. S. B., Halios, C. H., Hamilton, J. F., Harrison, R. M., Heal, M. R., Heard,  
771 D. E., Helfter, C., Herndon, S. C., Holmes, R. E., Hopkins, J. R., Jones, A. M., Kelly, F. J.,  
772 Kotthaus, S., Langford, B., Lee, J. D., Leigh, R. J., Lewis, A. C., Lidster, R. T., Lopez-Hilfiker,  
773 F. D., McQuaid, J. B., Mohr, C., Monks, P. S., Nemitz, E., Ng, N. L., Percival, C. J., Prévôt, A. S.  
774 H., Ricketts, H. M. A., Sokhi, R., Stone, D., Thornton, J. A., Tremper, A. H., Valach, A. C.,  
775 Visser, S., Whalley, L. K., Williams, L. R., Xu, L., Young, D. E., Zotter, P., Bohnenstengel, S. I.,  
776 Belcher, S. E., Aiken, A., Allan, J. D., Allen, G., Bacak, A., Bannan, T. J., Barlow, J. F.,  
777 Beddows, D. C. S., Bloss, W. J., Booth, A. M., Chemel, C., Coceal, O., Marco, C. F. D., Dubey,  
778 M. K., Faloon, K. H., Fleming, Z. L., Furger, M., Gietl, J. K., Graves, R. R., Green, D. C.,  
779 Grimmond, C. S. B., Halios, C. H., Hamilton, J. F., Harrison, R. M., Heal, M. R., Heard, D. E.,  
780 Helfter, C., Herndon, S. C., Holmes, R. E., Hopkins, J. R., Jones, A. M., Kelly, F. J., Kotthaus,  
781 S., Langford, B., Lee, J. D., Leigh, R. J., Lewis, A. C., Lidster, R. T., Lopez-Hilfiker, F. D., et al.:  
782 Meteorology, Air Quality, and Health in London: The ClearfLo Project, *Bull. Am. Meteorol.*

783 Soc., 96(5), 779–804, 2015.

784 Burnett, R., Chen, H., Szyszkowicz, M., Fann, N., Hubbell, B., Pope, C. A., Apte, J. S., Brauer,  
785 M., Cohen, A., Weichenthal, S., Coggins, J., Di, Q., Brunekreef, B., Frostad, J., Lim, S. S., Kan,  
786 H., Walker, K. D., Thurston, G. D., Hayes, R. B., Lim, C. C., Turner, M. C., Jerrett, M., Krewski,  
787 D., Gapstur, S. M., Diver, W. R., Ostro, B., Goldberg, D., Crouse, D. L., Martin, R. V., Peters, P.,  
788 Pinault, L., Tjepkema, M., van Donkelaar, A., Villeneuve, P. J., Miller, A. B., Yin, P., Zhou, M.,  
789 Wang, L., Janssen, N. A. H., Marra, M., Atkinson, R. W., Tsang, H., Quoc Thach, T., Cannon, J.  
790 B., Allen, R. T., Hart, J. E., Laden, F., Cesaroni, G., Forastiere, F., Weinmayr, G., Jaensch, A.,  
791 Nagel, G., Concin, H. and Spadaro, J. V.: Global estimates of mortality associated with long-term  
792 exposure to outdoor fine particulate matter, *Proc. Natl. Acad. Sci. U. S. A.*, 115(38), 9592–9597,  
793 2018.

794 Burnett, R. T., Pope, C. A., Ezzati, M., Olives, C., Lim, S. S., Mehta, S., Shin, H. H., Singh, G.,  
795 Hubbell, B., Brauer, M., Anderson, H. R., Smith, K. R., Balmes, J. R., Bruce, N. G., Kan, H.,  
796 Laden, F., Prüss-Ustün, A., Turner, M. C., Gapstur, S. M., Diver, W. R. and Cohen, A.: An  
797 integrated risk function for estimating the global burden of disease attributable to ambient fine  
798 particulate matter exposure, *Environ. Health Perspect.*, 122(4), 397–403, 2014.

799 Cappa, C. D., Jathar, S. H., Kleeman, M. J., Docherty, K. S., Jimenez, J. L., Seinfeld, J. H. and  
800 Wexler, A. S.: Simulating secondary organic aerosol in a regional air quality model using the  
801 statistical oxidation model - Part 2: Assessing the influence of vapor wall losses, *Atmos. Chem.*  
802 *Phys.*, 16(5), 3041–3059, 2016.

803 Chafe, Z., Brauer, M., Heroux, M.-E., Klimont, Z., Lanki, T., Salonen, R. O. and Smith, K. R.:  
804 Residential heating with wood and coal: Health impacts and policy options in Europe and North  
805 America, WHO/UNECE LRTAP., 2015.

806 CIESIN: Gridded Population of the World (GPW), v4, SEDAC [online] Available from:  
807 <https://sedac.ciesin.columbia.edu/data/collection/gpw-v4> (Accessed 12 May 2020), 2017.

808 Coggon, M. M., McDonald, B. C., Vlasenko, A., Veres, P. R., Bernard, F., Koss, A. R., Yuan, B.,  
809 Gilman, J. B., Peischl, J., Aikin, K. C., DuRant, J., Warneke, C., Li, S.-M. and de Gouw, J. A.:  
810 Diurnal Variability and Emission Pattern of Decamethylcyclopentasiloxane (D<sub>5</sub>) from the  
811 Application of Personal Care Products in Two North American Cities, *Environ. Sci. Technol.*,  
812 52(10), 5610–5618, 2018.

813 Cohen, A. J., Brauer, M., Burnett, R., Anderson, H. R., Frostad, J., Estep, K., Balakrishnan, K.,  
814 Brunekreef, B., Dandona, L., Dandona, R., Feigin, V., Freedman, G., Hubbell, B., Jobling, A.,  
815 Kan, H., Knibbs, L., Liu, Y., Martin, R., Morawska, L., Pope, C. A., Shin, H., Straif, K.,  
816 Shaddick, G., Thomas, M., van Dingenen, R., van Donkelaar, A., Vos, T., Murray, C. J. L. and  
817 Forouzanfar, M. H.: Estimates and 25-year trends of the global burden of disease attributable to  
818 ambient air pollution: an analysis of data from the Global Burden of Diseases Study 2015,  
819 *Lancet*, 389(10082), 1907–1918, 2017.

820 DeCarlo, P. F., Dunlea, E. J., Kimmel, J. R., Aiken, A. C., Sueper, D., Crounse, J., Wennberg, P.

821 O., Emmons, L., Shinozuka, Y., Clarke, A., Zhou, J., Tomlinson, J., Collins, D. R., Knapp, D.,  
822 Weinheimer, A. J., Montzka, D. D., Campos, T. and Jimenez, J. L.: Fast airborne aerosol size and  
823 chemistry measurements above Mexico City and Central Mexico during the MILAGRO  
824 campaign, *Atmos. Chem. Phys.*, 8(14), 4027–4048, 2008.

825 DeCarlo, P. F., Ulbrich, I. M., Crouse, J., de Foy, B., Dunlea, E. J., Aiken, A. C., Knapp, D.,  
826 Weinheimer, A. J., Campos, T., Wennberg, P. O. and Jimenez, J. L.: Investigation of the sources  
827 and processing of organic aerosol over the Central Mexican Plateau from aircraft measurements  
828 during MILAGRO, *Atmos. Chem. Phys.*, 10(12), 5257–5280, 2010.

829 Deming, B., Pagonis, D., Liu, X., Talukdar, R. K., Roberts, J. M., Veres, P. R., Krechmer, J. E.,  
830 de Gouw, J. A., Jimenez, J. L. and Ziemann, P. J.: Measurements of Delays of Gas-Phase  
831 Compounds in a Wide Variety of Tubing Materials due to Gas-Wall Partitioning, *Atmos. Meas.*  
832 *Tech.*, In Prep., 2018.

833 Dominutti, P., Keita, S., Bahino, J., Colomb, A., Lioussé, C., Yoboué, V., Galy-Lacaux, C.,  
834 Morris, E., Bouvier, L., Sauvage, S. and Borbon, A.: Anthropogenic VOCs in Abidjan, southern  
835 West Africa: from source quantification to atmospheric impacts, *Atmos. Chem. Phys.*, 19(18),  
836 11721–11741, 2019.

837 van Donkelaar, A., Martin, R. V., Brauer, M. and Boys, B. L.: Use of Satellite Observations for  
838 Long-Term Exposure Assessment of Global Concentrations of Fine Particulate Matter, *Environ.*  
839 *Health Perspect.*, 123(2), 135–143, 2015.

840 van Donkelaar, A., Martin, R. V., Brauer, M., Hsu, N. C., Kahn, R. A., Levy, R. C., Lyapustin,  
841 A., Sayer, A. M. and Winker, D. M.: Global Estimates of Fine Particulate Matter using a  
842 Combined Geophysical-Statistical Method with Information from Satellites, Models, and  
843 Monitors, *Environ. Sci. Technol.*, 50(7), 3762–3772, 2016.

844 Dzepina, K., Volkamer, R. M., Madronich, S., Tulet, P., Ulbrich, I. M., Zhang, Q., Cappa, C. D.,  
845 Ziemann, P. J. and Jimenez, J. L.: Evaluation of recently-proposed secondary organic aerosol  
846 models for a case study in Mexico City, *Atmos. Chem. Phys.*, 9(15), 5681–5709, 2009.

847 EMEP/EEA: EMEP/EEA Air Pollutant Emission Inventory Guidebook 2016, EEA,  
848 Luxembourg., 2016.

849 Ensberg, J. J., Hayes, P. L., Jimenez, J. L., Gilman, J. B., Kuster, W. C., de Gouw, J. A.,  
850 Holloway, J. S., Gordon, T. D., Jathar, S., Robinson, A. L. and Seinfeld, J. H.: Emission factor  
851 ratios, SOA mass yields, and the impact of vehicular emissions on SOA formation, *Atmos.*  
852 *Chem. Phys.*, 14(5), 2383–2397, 2014.

853 Freney, E. J., Sellegri, K., Canonaco, F., Colomb, A., Borbon, A., Michoud, V., Crumeyrolle, S.,  
854 Amarouche, N., Bourianne, T., Gomes, L., Prevot, A. S. H., Beekmann, M. and  
855 Schwarzenböeck, A.: Characterizing the impact of urban emissions on regional aerosol particles:  
856 Airborne measurements during the MEGAPOLI experiment, *Atmos. Chem. Phys.*, 14(3),  
857 1397–1412, 2014.

858 Gentner, D. R., Isaacman, G., Worton, D. R., Chan, A. W. H., Dallmann, T. R., Davis, L., Liu, S.,  
859 Day, D. A., Russell, L. M., Wilson, K. R., Weber, R., Guha, A., Harley, R. A. and Goldstein, A.  
860 H.: Elucidating secondary organic aerosol from diesel and gasoline vehicles through detailed  
861 characterization of organic carbon emissions, *Proc. Natl. Acad. Sci. U. S. A.*, 109(45),  
862 18318–18323, 2012.

863 Goel, R. and Guttikunda, S. K.: Evolution of on-road vehicle exhaust emissions in Delhi, *Atmos.*  
864 *Environ.*, 105, 78–90, 2015.

865 de Gouw, J. A. and Jimenez, J. L.: Organic Aerosols in the Earth's Atmosphere, *Environ. Sci.*  
866 *Technol.*, 43(20), 7614–7618, 2009.

867 de Gouw, J. A., Middlebrook, A. M., Warneke, C., Goldan, P. D., Kuster, W. C., Roberts, J. M.,  
868 Fehsenfeld, F. C., Worsnop, D. R., Canagaratna, M. R., Pszenny, A. A. P., Keene, W. C.,  
869 Marchewka, M., Bertman, S. B. and Bates, T. S.: Budget of organic carbon in a polluted  
870 atmosphere: Results from the New England Air Quality Study in 2002, *J. Geophys. Res. D:*  
871 *Atmos.*, 110(16), 1–22, 2005.

872 de Gouw, J. A., Gilman, J. B., Kim, S.-W., Lerner, B. M., Isaacman-VanWertz, G., McDonald, B.  
873 C., Warneke, C., Kuster, W. C., Lefer, B. L., Griffith, S. M., Dusanter, S., Stevens, P. S. and  
874 Stutz, J.: Chemistry of Volatile Organic Compounds in the Los Angeles basin: Nighttime  
875 Removal of Alkenes and Determination of Emission Ratios, *J. Geophys. Res.: Atmos.*, 122(21),  
876 11,843–11,861, 2017.

877 de Gouw, J. A., Gilman, J. B., Kim, S.-W., Alvarez, S. L., Dusanter, S., Graus, M., Griffith, S.  
878 M., Isaacman-VanWertz, G., Kuster, W. C., Lefer, B. L., Lerner, B. M., McDonald, B. C.,  
879 Rappenglück, B., Roberts, J. M., Stevens, P. S., Stutz, J., Thalman, R., Veres, P. R., Volkamer, R.,  
880 Warneke, C., Washenfelder, R. A. and Young, C. J.: Chemistry of volatile organic compounds in  
881 the Los Angeles basin: Formation of oxygenated compounds and determination of emission  
882 ratios, *J. Geophys. Res.*, 123(4), 2298–2319, 2018.

883 Grieshop, A. P., Logue, J. M., Donahue, N. M. and Robinson, A. L.: Laboratory investigation of  
884 photochemical oxidation of organic aerosol from wood fires 1: measurement and simulation of  
885 organic aerosol evolution, *Atmos. Chem. Phys.*, 9(4), 1263–1277, 2009.

886 Hallquist, M., Wenger, J. C., Baltensperger, U., Rudich, Y., Simpson, D., Claeys, M., Dommen,  
887 J., Donahue, N. M., George, C., Goldstein, A. H., Hamilton, J. F., Herrmann, H., Hoffmann, T.,  
888 Iinuma, Y., Jang, M., Jenkin, M. E., Jimenez, J. L., Kiendler-Scharr, A., Maenhaut, W.,  
889 McFiggans, G., Mentel, T. F., Monod, A., Prévôt, A. S. H., Seinfeld, J. H., Surratt, J. D.,  
890 Szmigielski, R. and Wildt, J.: The formation, properties and impact of secondary organic aerosol:  
891 current and emerging issues, *Atmos. Chem. Phys.*, 9(14), 5155–5236, 2009.

892 Hayes, P. L., Ortega, A. M., Cubison, M. J., Froyd, K. D., Zhao, Y., Cliff, S. S., Hu, W. W.,  
893 Toohey, D. W., Flynn, J. H., Lefer, B. L., Grossberg, N., Alvarez, S., Rappenglück, B., Taylor, J.  
894 W., Allan, J. D., Holloway, J. S., Gilman, J. B., Kuster, W. C., de Gouw, J. A., Massoli, P.,  
895 Zhang, X., Liu, J., Weber, R. J., Corrigan, A. L., Russell, L. M., Isaacman, G., Worton, D. R.,

896 Kreisberg, N. M., Goldstein, A. H., Thalman, R., Waxman, E. M., Volkamer, R., Lin, Y. H.,  
897 Surratt, J. D., Kleindienst, T. E., Offenberg, J. H., Dusanter, S., Griffith, S., Stevens, P. S.,  
898 Brioude, J., Angevine, W. M. and Jimenez, J. L.: Organic aerosol composition and sources in  
899 Pasadena, California, during the 2010 CalNex campaign, *J. Geophys. Res. D: Atmos.*, 118(16),  
900 9233–9257, 2013.

901 Hayes, P. L., Carlton, A. G., Baker, K. R., Ahmadov, R., Washenfelder, R. A., Alvarez, S.,  
902 Rappenglück, B., Gilman, J. B., Kuster, W. C., de Gouw, J. A., Zotter, P., Prévôt, A. S. H.,  
903 Szidat, S., Kleindienst, T. E., Ma, P. K. and Jimenez, J. L.: Modeling the formation and aging of  
904 secondary organic aerosols in Los Angeles during CalNex 2010, *Atmos. Chem. Phys.*, 15(10),  
905 5773–5801, 2015.

906 Heringa, M. F., DeCarlo, P. F., Chirico, R., Tritscher, T., Dommen, J., Weingartner, E., Richter,  
907 R., Wehrle, G., Prévôt, A. S. H. and Baltensperger, U.: Investigations of primary and secondary  
908 particulate matter of different wood combustion appliances with a high-resolution time-of-flight  
909 aerosol mass spectrometer, *Atmos. Chem. Phys.*, 11(12), 5945–5957, 2011.

910 Herndon, S. C., Onasch, T. B., Wood, E. C., Kroll, J. H., Canagaratna, M. R., Jayne, J. T.,  
911 Zavala, M. A., Knighton, W. B., Mazzoleni, C., Dubey, M. K., Ulbrich, I. M., Jimenez, J. L.,  
912 Seila, R., de Gouw, J. A., de Foy, B., Fast, J., Molina, L. T., Kolb, C. E. and Worsnop, D. R.:  
913 Correlation of secondary organic aerosol with odd oxygen in Mexico City, *Geophys. Res. Lett.*,  
914 35(15), L15804, 2008.

915 Hodzic, A. and Jimenez, J. L.: Modeling anthropogenically controlled secondary organic  
916 aerosols in a megacity: A simplified framework for global and climate models, *Geosci. Model*  
917 *Dev.*, 4(4), 901–917, 2011.

918 Hodzic, A., Jimenez, J. L., Madronich, S., Aiken, A. C., Bessagnet, B., Curci, G., Fast, J.,  
919 Lamarque, J.-F., Onasch, T. B., Roux, G., Schauer, J. J., Stone, E. A. and Ulbrich, I. M.:  
920 Modeling organic aerosols during MILAGRO: importance of biogenic secondary organic  
921 aerosols, *Atmos. Chem. Phys.*, 9(18), 6949–6981, 2009.

922 Hodzic, A., Jimenez, J. L., Prévôt, A. S. H., Szidat, S., Fast, J. D. and Madronich, S.: Can 3-D  
923 models explain the observed fractions of fossil and non-fossil carbon in and near Mexico City?,  
924 *Atmos. Chem. Phys.*, 10(22), 10997–11016, 2010a.

925 Hodzic, A., Jimenez, J. L., Madronich, S., Canagaratna, M. R., DeCarlo, P. F., Kleinman, L. and  
926 Fast, J.: Modeling organic aerosols in a megacity: potential contribution of semi-volatile and  
927 intermediate volatility primary organic compounds to secondary organic aerosol formation,  
928 *Atmos. Chem. Phys.*, 10(12), 5491–5514, 2010b.

929 Hodzic, A., Campuzano-Jost, P., Bian, H., Chin, M., Colarco, P. R., Day, D. A., Froyd, K. D.,  
930 Heinold, B., Jo, D. S., Katich, J. M., Kodros, J. K., Nault, B. A., Pierce, J. R., Ray, E., Schacht,  
931 J., Schill, G. P., Schroder, J. C., Schwarz, J. P., Sueper, D. T., Tegen, I., Tilmes, S., Tsigaridis, K.,  
932 Yu, P. and Jimenez, J. L.: Characterization of Organic Aerosol across the Global Remote  
933 Troposphere: A comparison of ATOM measurements and global chemistry models, *Atmos.*

934 Chem. Phys., 20(8), 4607–4635, 2020.

935 Hu, W., Hu, M., Hu, W., Jimenez, J. L., Yuan, B., Chen, W., Wang, M., Wu, Y., Chen, C., Wang,  
936 Z., Peng, J., Zeng, L. and Shao, M.: Chemical composition, sources, and aging process of  
937 submicron aerosols in Beijing: Contrast between summer and winter, J. Geophys. Res. D:  
938 Atmos., 121(4), 1955–1977, 2016.

939 Hu, W., Downward, G., Wong, J. Y. Y., Reiss, B., Rothman, N., Portengen, L., Li, J., Jones, R.  
940 R., Huang, Y., Yang, K., Chen, Y., Xu, J., He, J., Bassig, B., Seow, W. J., Hosgood, H. D., Zhang,  
941 L., Wu, G., Wei, F., Vermeulen, R. and Lan, Q.: Characterization of outdoor air pollution from  
942 solid fuel combustion in Xuanwei and Fuyuan, a rural region of China, Sci. Rep., 10(1), 11335,  
943 2020.

944 Hu, W. W., Hu, M., Yuan, B., Jimenez, J. L., Tang, Q., Peng, J. F., Hu, W., Shao, M., Wang, M.,  
945 Zeng, L. M., Wu, Y. S., Gong, Z. H., Huang, X. F. and He, L. Y.: Insights on organic aerosol  
946 aging and the influence of coal combustion at a regional receptor site of central eastern China,  
947 Atmos. Chem. Phys., 13(19), 10095–10112, 2013.

948 IHME: Global Burden of Disease Study 2015 (GBD 2015) Data Resources, GHDx [online]  
949 Available from: <http://ghdx.healthdata.org/gbd-2015> (Accessed 2019), 2016.

950 Janssen, R. H. H., Tsimpidi, A. P., Karydis, V. A., Pozzer, A., Lelieveld, J., Crippa, M., Prévôt,  
951 A. S. H., Ait-Helal, W., Borbon, A., Sauvage, S. and Locoge, N.: Influence of local production  
952 and vertical transport on the organic aerosol budget over Paris, J. Geophys. Res. D: Atmos.,  
953 122(15), 8276–8296, 2017.

954 Janssens-Maenhout, G., Crippa, M., Guizzardi, D., Dentener, F., Muntean, M., Pouliot, G.,  
955 Keating, T., Zhang, Q., Kurokawa, J., Wankmüller, R., Denier van der Gon, H., Kuenen, J. J. P.,  
956 Klimont, Z., Frost, G., Darras, S., Koffi, B. and Li, M.: HTAP\_v2.2: a mosaic of regional and  
957 global emission grid maps for 2008 and 2010 to study hemispheric transport of air pollution,  
958 Atmos. Chem. Phys., 15(19), 11411–11432, 2015.

959 Jathar, S. H., Woody, M., Pye, H. O. T., Baker, K. R. and Robinson, A. L.: Chemical transport  
960 model simulations of organic aerosol in southern California: model evaluation and gasoline and  
961 diesel source contributions, Atmos. Chem. Phys., 17(6), 4305–4318, 2017.

962 Jena, C., Ghude, S. D., Kulkarni, R., Debnath, S., Kumar, R., Soni, V. K., Acharja, P., Kulkarni,  
963 S. H., Khare, M., Kaginalkar, A. J., Chate, D. M., Ali, K., Nanjundiah, R. S. and Rajeevan, M.  
964 N.: Evaluating the sensitivity of fine particulate matter (PM<sub>2.5</sub>) simulations to chemical  
965 mechanism in Delhi, Atmos. Chem. Phys. Discuss., doi:10.5194/acp-2020-673, 2020.

966 Jimenez, J. L., Canagaratna, M. R., Donahue, N. M., Prevot, A. S. H., Zhang, Q., Kroll, J. H.,  
967 DeCarlo, P. F., Allan, J. D., Coe, H., Ng, N. L., Aiken, A. C., Docherty, K. S., Ulbrich, I. M.,  
968 Grieshop, A. P., Robinson, A. L., Duplissy, J., Smith, J. D., Wilson, K. R., Lanz, V. A., Hueglin,  
969 C., Sun, Y. L., Tian, J., Laaksonen, A., Raatikainen, T., Rautiainen, J., Vaattovaara, P., Ehn, M.,  
970 Kulmala, M., Tomlinson, J. M., Collins, D. R., Cubison, M. J., Dunlea, E. J., Huffman, J. A.,

971 Onasch, T. B., Alfarra, M. R., Williams, P. I., Bower, K., Kondo, Y., Schneider, J., Drewnick, F.,  
972 Borrmann, S., Weimer, S., Demerjian, K., Salcedo, D., Cottrell, L., Griffin, R., Takami, A.,  
973 Miyoshi, T., Hatakeyama, S., Shimono, A., Sun, J. Y., Zhang, Y. M., Dzepina, K., Kimmel, J. R.,  
974 Sueper, D., Jayne, J. T., Herndon, S. C., Trimborn, A. M., Williams, L. R., Wood, E. C.,  
975 Middlebrook, A. M., Kolb, C. E., Baltensperger, U. and Worsnop, D. R.: Evolution of organic  
976 aerosols in the atmosphere, *Science*, 326(5959), 1525–1529, 2009.

977 Khare, P. and Gentner, D. R.: Considering the future of anthropogenic gas-phase organic  
978 compound emissions and the increasing influence of non-combustion sources on urban air  
979 quality, *Atmos. Chem. Phys.*, 18(8), 5391–5413, 2018.

980 Khare, P., Machesky, J., Soto, R., He, M., Presto, A. A. and Gentner, D. R.: Asphalt-related  
981 emissions are a major missing nontraditional source of secondary organic aerosol precursors, *Sci*  
982 *Adv*, 6(36), doi:10.1126/sciadv.abb9785, 2020.

983 Kleinman, L. I., Daum, P. H., Lee, Y.-N., Senum, G. I., Springston, S. R., Wang, J., Berkowitz,  
984 C., Hubbe, J., Zaveri, R. A., Brechtel, F. J., Jayne, J., Onasch, T. B. and Worsnop, D.: Aircraft  
985 observations of aerosol composition and ageing in New England and Mid-Atlantic States during  
986 the summer 2002 New England Air Quality Study field campaign, *J. Geophys. Res. D: Atmos.*,  
987 112(D9), D09310, 2007.

988 Kodros, J. K., Carter, E., Brauer, M., Volckens, J., Bilsback, K. R., L'Orange, C., Johnson, M.  
989 and Pierce, J. R.: Quantifying the Contribution to Uncertainty in Mortality Attributed to  
990 Household, Ambient, and Joint Exposure to PM<sub>2.5</sub> From Residential Solid Fuel Use, *Geohealth*,  
991 2(1), 25–39, 2018.

992 Kodros, J. K., Papanastasiou, D. K., Paglione, M., Masiol, M., Squizzato, S., Florou, K.,  
993 Skyllakou, K., Kaltsonoudis, C., Nenes, A. and Pandis, S. N.: Rapid dark aging of biomass  
994 burning as an overlooked source of oxidized organic aerosol, *Proc. Natl. Acad. Sci. U. S. A.*,  
995 117(52), 33028–33033, 2020.

996 Kondo, Y., Morino, Y., Fukuda, M., Kanaya, Y., Miyazaki, Y., Takegawa, N., Tanimoto, H.,  
997 McKenzie, R., Johnston, P., Blake, D. R., Murayama, T. and Koike, M.: Formation and transport  
998 of oxidized reactive nitrogen, ozone, and secondary organic aerosol in Tokyo, *J. Geophys. Res.*  
999 *D: Atmos.*, 113(D21), D21310, 2008.

1000 Krechmer, J. E., Pagonis, D., Ziemann, P. J. and Jimenez, J. L.: Quantification of Gas-Wall  
1001 Partitioning in Teflon Environmental Chambers Using Rapid Bursts of Low-Volatility Oxidized  
1002 Species Generated in Situ, *Environ. Sci. Technol.*, 50(11), 5757–5765, 2016.

1003 Krewski, D., Jerrett, M., Burnett, R. T., Ma, R., Hughes, E., Shi, Y., Turner, M. C., Arden, C.,  
1004 Thurston, G., Calle, E. E., Thun, M. J., Beckerman, B., Deluca, P., Finkelstein, N., Ito, K.,  
1005 Moore, D. K., Newbold, K. B., Ramsay, T., Ross, Z., Shin, H. and Tempalski, B.: Extended  
1006 Follow-Up and Spatial Analysis of the American Cancer Society Study Linking Particulate Air  
1007 Pollution and Mortality Number 140 May 2009 PRESS VERSION., 2009.



1008 Lacey, F. G., Henze, D. K., Lee, C. J., van Donkelaar, A. and Martin, R. V.: Transient climate  
1009 and ambient health impacts due to national solid fuel cookstove emissions, *Proc. Natl. Acad. Sci.*  
1010 *U. S. A.*, 114(6), 1269–1274, 2017.

1011 Lam, N. L., Upadhyay, B., Maharjan, S., Jagoe, K., Weyant, C. L., Thompson, R., Uprety, S.,  
1012 Johnson, M. A. and Bond, T. C.: Seasonal fuel consumption, stoves, and end-uses in rural  
1013 households of the far-western development region of Nepal, *Environ. Res. Lett.*, 12(12), 125011,  
1014 2017.

1015 Landrigan, P. J., Fuller, R., Acosta, N. J. R., Adeyi, O., Arnold, R., Basu, N., Baldé, A. B.,  
1016 Bertollini, R., Bose-O'Reilly, S., Boufford, J. I., Breyse, P. N., Chiles, T., Mahidol, C.,  
1017 Coll-Seck, A. M., Cropper, M. L., Fobil, J., Fuster, V., Greenstone, M., Haines, A., Hanrahan, D.,  
1018 Hunter, D., Khare, M., Krupnick, A., Lanphear, B., Lohani, B., Martin, K., Mathiasen, K. V.,  
1019 McTeer, M. A., Murray, C. J. L., Ndahimananjara, J. D., Perera, F., Potočnik, J., Preker, A. S.,  
1020 Ramesh, J., Rockström, J., Salinas, C., Samson, L. D., Sandilya, K., Sly, P. D., Smith, K. R.,  
1021 Steiner, A., Stewart, R. B., Suk, W. A., van Schayck, O. C. P., Yadama, G. N., Yumkella, K. and  
1022 Zhong, M.: The Lancet Commission on pollution and health, *Lancet*, 391(10119), 462–512,  
1023 2018.

1024 Lelieveld, J., Evans, J. S., Fnais, M., Giannadaki, D. and Pozzer, A.: The contribution of outdoor  
1025 air pollution sources to premature mortality on a global scale, *Nature*, 525(7569), 367–371, 2015.

1026 Liao, J., Hanisco, T. F., Wolfe, G. M., St. Clair, J., Jimenez, J. L., Campuzano-Jost, P., Nault, B.  
1027 A., Fried, A., Marais, E. A., Gonzalez Abad, G., Chance, K., Jethva, H. T., Ryerson, T. B.,  
1028 Warneke, C. and Wisthaler, A.: Towards a satellite formaldehyde – in situ hybrid estimate for  
1029 organic aerosol abundance, *Atmos. Chem. Phys.*, 19(5), 2765–2785, 2019.

1030 Li, M., Zhang, Q., Zheng, B., Tong, D., Lei, Y., Liu, F., Chaopeng, H., Kang, S., Yan, L., Zhang,  
1031 Y., Bo, Y., Su, H., Cheng, Y. and He, K.: Persistent growth of anthropogenic non-methane  
1032 volatile organic compound (NMVOC) emissions in China during 1990-2017: drivers, speciation  
1033 and ozone formation potential, *Atmos. Chem. Phys.*, 19, 8897–8913, 2019.

1034 Liu, X., Deming, B., Pagonis, D., Day, D. A., Palm, B. B., Talukdar, R., Roberts, J. M., Veres, P.  
1035 R., Krechmer, J. E., Thornton, J. A., de Gouw, J. A., Ziemann, P. J. and Jimenez, J. L.: Effects of  
1036 gas–wall interactions on measurements of semivolatile compounds and small polar molecules, ,  
1037 doi:10.5194/amt-12-3137-2019, 2019.

1038 Lu, Q., Zhao, Y. and Robinson, A. L.: Comprehensive organic emission profiles for gasoline,  
1039 diesel, and gas-turbine engines including intermediate and semi-volatile organic compound  
1040 emissions, *Atmos. Chem. Phys.*, 18, 17637–17654, 2018.

1041 Ma, P. K., Zhao, Y., Robinson, A. L., Worton, D. R., Goldstein, A. H., Ortega, A. M., Jimenez, J.  
1042 L., Zotter, P., Prévôt, A. S. H., Szidat, S. and Hayes, P. L.: Evaluating the impact of new  
1043 observational constraints on P-S/IVOC emissions, multi-generation oxidation, and chamber wall  
1044 losses on SOA modeling for Los Angeles, CA, *Atmos. Chem. Phys.*, 17(15), 9237–9259, 2017.

1045 McDonald, B. C., de Gouw, J. A., Gilman, J. B., Jathar, S. H., Akherati, A., Cappa, C. D.,  
1046 Jimenez, J. L., Lee-Taylor, J., Hayes, P. L., McKeen, S. A., Cui, Y. Y., Kim, S.-W., Gentner, D.  
1047 R., Isaacman-VanWertz, G., Goldstein, A. H., Harley, R. A., Frost, G. J., Roberts, J. M., Ryerson,  
1048 T. B. and Trainer, M.: Volatile chemical products emerging as largest petrochemical source of  
1049 urban organic emissions, *Science*, 359(6377), 760–764, 2018.

1050 Miyakawa, T., Takegawa, N. and Kondo, Y.: Photochemical evolution of submicron aerosol  
1051 chemical composition in the Tokyo megacity region in summer, *J. Geophys. Res. D: Atmos.*,  
1052 113(D14), D14304, 2008.

1053 Molina, L. T., Kolb, C. E., de Foy, B., Lamb, B. K., Brune, W. H., Jimenez, J. L.,  
1054 Ramos-Villegas, R., Sarmiento, J., Paramo-Figueroa, V. H., Cardenas, B., Gutierrez-Avedoy, V.  
1055 and Molina, M. J.: Air quality in North America's most populous city – overview of the  
1056 MCMA-2003 campaign, *Atmos. Chem. Phys.*, 7(10), 2447–2473, 2007.

1057 Molina, L. T., Madronich, S., Gaffney, J. S., Apel, E., de Foy, B., Fast, J., Ferrare, R., Herndon,  
1058 S., Jimenez, J. L., Lamb, B., Osornio-Vargas, A. R., Russell, P., Schauer, J. J., Stevens, P. S.,  
1059 Volkamer, R. and Zavala, M.: An overview of the MILAGRO 2006 Campaign: Mexico City  
1060 emissions and their transport and transformation, *Atmos. Chem. Phys.*, 10(18), 8697–8760,  
1061 2010.

1062 Morino, Y., Tanabe, K., Sato, K. and Ohara, T.: Secondary organic aerosol model  
1063 intercomparison based on secondary organic aerosol to odd oxygen ratio in Tokyo, *J. Geophys.*  
1064 *Res.: Atmos.*, 119(23), 13,489–13,505, 2014.

1065 Murphy, B. N., Woody, M. C., Jimenez, J. L., Carlton, A. M. G., Hayes, P. L., Liu, S., Ng, N. L.,  
1066 Russell, L. M., Setyan, A., Xu, L., Young, J., Zaveri, R. A., Zhang, Q. and Pye, H. O. T.:  
1067 Semivolatile POA and parameterized total combustion SOA in CMAQv5.2: impacts on source  
1068 strength and partitioning, *Atmos. Chem. Phys.*, 17(18), 11107–11133, 2017.

1069 Nault, B. A., Campuzano-Jost, P., Day, D. A., Schroder, J. C., Anderson, B., Beyersdorf, A. J.,  
1070 Blake, D. R., Brune, W. H., Choi, Y., Corr, C. A., de Gouw, J. A., Dibb, J., DiGangi, J. P., Diskin,  
1071 G. S., Fried, A., Huey, L. G., Kim, M. J., Knute, C. J., Lamb, K. D., Lee, T., Park, T., Pusede, S.  
1072 E., Scheuer, E., Thornhill, K. L., Woo, J.-H. and Jimenez, J. L.: Secondary Organic Aerosol  
1073 Production from Local Emissions Dominates the Organic Aerosol Budget over Seoul, South  
1074 Korea, during KORUS-AQ, *Atmos. Chem. Phys.*, 18, 17769–17800, 2018.

1075 Pagonis, D., Krechmer, J. E., de Gouw, J., Jimenez, J. L. and Ziemann, P. J.: Effects of Gas-Wall  
1076 Partitioning in Teflon Tubing and Instrumentation on Time-Resolved Measurements of  
1077 Gas-Phase Organic Compounds, *Atmospheric Measurement Techniques Discussions*, 1–19,  
1078 2017.

1079 Pai, S. J., Heald, C. L., Pierce, J. R., Farina, S. C., Marais, E. A., Jimenez, J. L.,  
1080 Campuzano-Jost, P., Nault, B. A., Middlebrook, A. M., Coe, H., Shilling, J. E., Bahreini, R.,  
1081 Dingle, J. H. and Vu, K.: An evaluation of global organic aerosol schemes using airborne

1082 observations, *Atmos. Chem. Phys.*, 20(5), 2637–2665, 2020.

1083 Parrish, D. D., Kuster, W. C., Shao, M., Yokouchi, Y., Kondo, Y., Goldan, P. D., de Gouw, J. A.,  
1084 Koike, M. and Shirai, T.: Comparison of air pollutant emissions among mega-cities, *Atmos.*  
1085 *Environ.*, 43(40), 6435–6441, 2009.

1086 Petit, J.-E., Favez, O., Sciare, J., Canonaco, F., Croteau, P., Močnik, G., Jayne, J., Worsnop, D.  
1087 and Leoz-Garziandia, E.: Submicron aerosol source apportionment of wintertime pollution in  
1088 Paris, France by double positive matrix factorization (PMF<sup>2</sup>) using an aerosol chemical  
1089 speciation monitor (ACSM) and a multi-wavelength Aethalometer, *Atmos. Chem. Phys.*, 14(24),  
1090 13773–13787, 2014.

1091 Platt, S. M., Haddad, I. E., Pieber, S. M., Huang, R.-J., Zardini, A. A., Clairotte, M.,  
1092 Suarez-Bertoa, R., Barmet, P., Pfaffenberger, L., Wolf, R., Slowik, J. G., Fuller, S. J., Kalberer,  
1093 M., Chirico, R., Dommen, J., Astorga, C., Zimmermann, R., Marchand, N., Hellebust, S.,  
1094 Temime-Roussel, B., Baltensperger, U. and Prévôt, A. S. H.: Two-stroke scooters are a dominant  
1095 source of air pollution in many cities, *Nat. Commun.*, 5(1), 3749, 2014.

1096 Pollack, I. B., Ryerson, T. B., Trainer, M., Neuman, J. A., Roberts, J. M. and Parrish, D. D.:  
1097 Trends in ozone, its precursors, and related secondary oxidation products in Los Angeles,  
1098 California: A synthesis of measurements from 1960 to 2010, *J. Geophys. Res. D: Atmos.*,  
1099 118(11), 5893–5911, 2013.

1100 Pungler, E. M. and West, J. J.: The effect of grid resolution on estimates of the burden of ozone  
1101 and fine particulate matter on premature mortality in the USA, *Air Qual. Atmos. Health*, 6(3),  
1102 563–573, 2013.

1103 Ridley, D. A., Heald, C. L., Ridley, K. J. and Kroll, J. H.: Causes and consequences of  
1104 decreasing atmospheric organic aerosol in the United States, *Proc. Natl. Acad. Sci. U. S. A.*,  
1105 115(2), 290–295, 2018.

1106 Robinson, A. L., Donahue, N. M., Shrivastava, M. K., Weitkamp, E. A., Sage, A. M., Grieshop,  
1107 A. P., Lane, T. E., Pierce, J. R. and Pandis, S. N.: Rethinking Organic Aerosols: Semivolatile  
1108 Emissions and Photochemical Aging, *Science*, 315(5816), 1259–1262, 2007.

1109 Ryerson, T. B., Andrews, A. E., Angevine, W. M., Bates, T. S., Brock, C. A., Cairns, B., Cohen,  
1110 R. C., Cooper, O. R., de Gouw, J. A., Fehsenfeld, F. C., Ferrare, R. A., Fischer, M. L., Flagan, R.  
1111 C., Goldstein, A. H., Hair, J. W., Hardesty, R. M., Hostetler, C. A., Jimenez, J. L., Langford, A.  
1112 O., McCauley, E., McKeen, S. A., Molina, L. T., Nenes, A., Oltmans, S. J., Parrish, D. D.,  
1113 Pederson, J. R., Pierce, R. B., Prather, K., Quinn, P. K., Seinfeld, J. H., Senff, C. J., Sorooshian,  
1114 A., Stutz, J., Surratt, J. D., Trainer, M., Volkamer, R., Williams, E. J. and Wofsy, S. C.: The 2010  
1115 California Research at the Nexus of Air Quality and Climate Change (CalNex) field study, *J.*  
1116 *Geophys. Res. D: Atmos.*, 118(11), 5830–5866, 2013.

1117 Sacks, J., Buckley, B., Alexis, N., Angrish, M., Beardslee, R., Benson, A., Brown, J., Buckley,  
1118 B., Campen, M., Chan, E., Coffman, E., Davis, A., Dutton, S. J., Eftim, S., Gandy, J., Hemming,

1119 B. L., Hines, E., Holliday, K., Kerminen, V.-M., Kiomourtzoglou, M.-A., Kirrane, E., Kotchmar,  
1120 D., Koturbash, I., Kulmala, M., Lassiter, M., Limaye, V., Ljungman, P., Long, T., Luben, T.,  
1121 Malm, W., McDonald, J. F., McDow, S., Mickley, L., Mikati, I., Mulholland, J., Nichols, J.,  
1122 Patel, M. M., Pinder, R., Pinto, J. P., Rappazzo, K., Richomond-Bryant, J., Rosa, M., Russell, A.,  
1123 Schichtel, B., Stewart, M., Stanek, L. W., Turner, M., Van Winkle, L., Wagner, J., Weaver,  
1124 Christopher, Wellenius, G., Whitsel, E., Yeckel, C., Zanobetti, A. and Zhang, M.: Integrated  
1125 Science Assessment (ISA) for Particulate Matter (Final Report, Dec 2019), Environmental  
1126 Protection Agency. [online] Available from:  
1127 <https://cfpub.epa.gov/ncea/isa/recordisplay.cfm?deid=347534> (Accessed 20 October 2020),  
1128 2019.

1129 Schroder, J. C., Campuzano-Jost, P., Day, D. A., Shah, V., Larson, K., Sommers, J. M., Sullivan,  
1130 A. P., Campos, T., Reeves, J. M., Hills, A., Hornbrook, R. S., Blake, N. J., Scheuer, E., Guo, H.,  
1131 Fibiger, D. L., McDuffie, E. E., Hayes, P. L., Weber, R. J., Dibb, J. E., Apel, E. C., Jaeglé, L.,  
1132 Brown, S. S., Thornton, J. A. and Jimenez, J. L.: Sources and Secondary Production of Organic  
1133 Aerosols in the Northeastern US during WINTER, *J. Geophys. Res. D: Atmos.*,  
1134 doi:10.1029/2018JD028475, 2018.

1135 Seinfeld, J. H. and Pandis, S. N.: *Atmospheric Chemistry and Physics: From Air Pollution to*  
1136 *Climate Change, Second.*, John Wiley & Sons, Inc., Hoboken, NJ USA., 2006.

1137 Seltzer, K. M., Pennington, E., Rao, V., Murphy, B. N., Strum, M., Isaacs, K. K. and Pye, H. O.  
1138 T.: Reactive organic carbon emissions from volatile chemical products, *Atmos. Chem. Phys.*, 21,  
1139 5079–5100, 2021.

1140 Shaddick, G., Thomas, M. L., Amini, H., Broday, D., Cohen, A., Frostad, J., Green, A., Gumy,  
1141 S., Liu, Y., Martin, R. V., Pruss-Ustun, A., Simpson, D., van Donkelaar, A. and Brauer, M.: Data  
1142 Integration for the Assessment of Population Exposure to Ambient Air Pollution for Global  
1143 Burden of Disease Assessment, *Environ. Sci. Technol.*, 52(16), 9069–9078, 2018.

1144 Shah, V., Jaeglé, L., Thornton, J. A., Lopez-Hilfiker, F. D., Lee, B. H., Schroder, J. C.,  
1145 Campuzano-Jost, P., Jimenez, J. L., Guo, H., Sullivan, A. P., Weber, R. J., Green, J. R., Fiddler,  
1146 M. N., Bililign, S., Campos, T. L., Stell, M., Weinheimer, A. J., Montzka, D. D. and Brown, S.  
1147 S.: Chemical feedbacks weaken the wintertime response of particulate sulfate and nitrate to  
1148 emissions reductions over the eastern United States, *Proc. Natl. Acad. Sci. U. S. A.*, 115(32),  
1149 8110–8115, 2018.

1150 Shah, V., Jaeglé, L., Jimenez, J. L., Schroder, J. C., Campuzano-Jost, P., Campos, T. L., Reeves,  
1151 J. M., Stell, M., Brown, S. S., Lee, B. H., Lopez-Hilfiker, F. D. and Thornton, J. A.: Widespread  
1152 Pollution from Secondary Sources of Organic Aerosols during Winter in the Northeastern United  
1153 States, *Geophys. Res. Lett.*, doi:10.1029/2018GL081530, 2019.

1154 Shrivastava, M., Cappa, C. D., Fan, J., Goldstein, A. H., Guenther, A. B., Jimenez, J. L., Kuang,  
1155 C., Laskin, A., Martin, S. T., Ng, N. L., Petaja, T., Pierce, J. R., Rasch, P. J., Roldin, P., Seinfeld,  
1156 J. H., Shilling, J., Smith, J. N., Thornton, J. A., Volkamer, R., Wang, J., Worsnop, D. R., Zaveri,  
1157 R. A., Zelenyuk, A. and Zhang, Q.: Recent advances in understanding secondary organic aerosol:

- 1158 Implications for global climate forcing, *Rev. Geophys.*, 55(2), 509–559, 2017.
- 1159 Silva, R. A., Adelman, Z., Fry, M. M. and West, J. J.: The Impact of Individual Anthropogenic  
1160 Emissions Sectors on the Global Burden of Human Mortality due to Ambient Air Pollution,  
1161 *Environ. Health Perspect.*, 124(11), 1776–1784, 2016.
- 1162 Singh, A., Satish, R. V. and Rastogi, N.: Characteristics and sources of fine organic aerosol over  
1163 a big semi-arid urban city of western India using HR-ToF-AMS, *Atmos. Environ.*, 208, 103–112,  
1164 2019.
- 1165 Stavroulas, I., Bougiatioti, A., Grivas, G., Paraskevopoulou, D., Tsagkaraki, M., Zarnpas, P.,  
1166 Liakakou, E., Gerasopoulos, E. and Mihalopoulos, N.: Sources and processes that control the  
1167 submicron organic aerosol composition in an urban Mediterranean environment (Athens): a high  
1168 temporal-resolution chemical composition measurement study, *Atmos. Chem. Phys.*, 19(2),  
1169 901–919, 2019.
- 1170 Stewart, G. J., Nelson, B. S., Acton, W. J. F., Vaughan, A. R., Farren, N. J., Hopkins, J. R., Ward,  
1171 M. W., Swift, S. J., Arya, R., Mondal, A., Jangirh, R., Ahlawat, S., Yadav, L., Sharma, S. K.,  
1172 Yunus, S. S. M., Hewitt, C. N., Nemitz, E., Mullinger, N., Gadi, R., Sahu, L. K., Tripathi, N.,  
1173 Rickard, A. R., Lee, J. D., Mandal, T. K. and Hamilton, J. F.: Emissions of intermediate-volatility  
1174 and semi-volatile organic compounds from domestic fuels used in Delhi, India, *Atmos. Chem.*  
1175 *Phys. Discuss.*, doi:10.5194/acp-2020-860, 2020.
- 1176 Toon, O. B., Maring, H., Dibb, J., Ferrare, R., Jacob, D. J., Jensen, E. J., Luo, Z. J., Mace, G. G.,  
1177 Pan, L. L., Pfister, L., Rosenlof, K. H., Redemann, J., Reid, J. S., Singh, H. B., Thompson, A.  
1178 M., Yokelson, R., Minnis, P., Chen, G., Jucks, K. W. and Pszenny, A.: Planning, implementation,  
1179 and scientific goals of the Studies of Emissions and Atmospheric Composition, Clouds and  
1180 Climate Coupling by Regional Surveys (SEAC<sup>4</sup>RS) field mission, *J. Geophys. Res. D: Atmos.*,  
1181 121(9), 4967–5009, 2016.
- 1182 Tsimpidi, A. P., Karydis, V. A., Zavala, M., Lei, W., Molina, L., Ulbrich, I. M., Jimenez, J. L. and  
1183 Pandis, S. N.: Evaluation of the volatility basis-set approach for the simulation of organic aerosol  
1184 formation in the Mexico City metropolitan area, *Atmos. Chem. Phys.*, 10(2), 525–546, 2010.
- 1185 Volkamer, R., Jimenez, J. L., San Martini, F., Dzepina, K., Zhang, Q., Salcedo, D., Molina, L. T.,  
1186 Worsnop, D. R. and Molina, M. J.: Secondary organic aerosol formation from anthropogenic air  
1187 pollution: Rapid and higher than expected, *Geophys. Res. Lett.*, 33(17), L17811, 2006.
- 1188 Wang, L., Slowik, J. G., Tripathi, N., Bhattu, D., Rai, P., Kumar, V., Vats, P., Satish, R.,  
1189 Baltensperger, U., Ganguly, D., Rastogi, N., Sahu, L. K., Tripathi, S. N. and Prévôt, A. S. H.:  
1190 Source characterization of volatile organic compounds measured by proton-transfer-reaction  
1191 time-of-flight mass spectrometers in Delhi, India, *Atmos. Chem. Phys.*, 20(16), 9753–9770,  
1192 2020.
- 1193 Warneke, C., de Gouw, J. A., Holloway, J. S., Peischl, J., Ryerson, T. B., Atlas, E., Blake, D.,  
1194 Trainer, M. and Parrish, D. D.: Multiyear trends in volatile organic compounds in Los Angeles,

1195 California: Five decades of decreasing emissions, *J. Geophys. Res. D: Atmos.*, 117(D21),  
1196 D00V17, 2012.

1197 Wood, E. C., Canagaratna, M. R., Herndon, S. C., Onasch, T. B., Kolb, C. E., Worsnop, D. R.,  
1198 Kroll, J. H., Knighton, W. B., Seila, R., Zavala, M., Molina, L. T., Decarlo, P. F., Jimenez, J. L.,  
1199 Weinheimer, A. J., Knapp, D. J., Jobson, B. T., Stutz, J., Kuster, W. C. and Williams, E. J.:  
1200 Investigation of the correlation between odd oxygen and secondary organic aerosol in Mexico  
1201 City and Houston, *Atmos. Chem. Phys.*, 10(18), 8947–8968, 2010.

1202 Woody, M. C., Baker, K. R., Hayes, P. L., Jimenez, J. L., Koo, B. and Pye, H. O. T.:  
1203 Understanding sources of organic aerosol during CalNex-2010 using the CMAQ-VBS, *Atmos.*  
1204 *Chem. Phys.*, 16(6), 4081–4100, 2016.

1205 Worton, D. R., Isaacman, G., Gentner, D. R., Dallmann, T. R., Chan, A. W. H., Ruehl, C.,  
1206 Kirchstetter, T. W., Wilson, K. R., Harley, R. A. and Goldstein, A. H.: Lubricating Oil Dominates  
1207 Primary Organic Aerosol Emissions from Motor Vehicles, *Environ. Sci. Technol.*, 48(7),  
1208 3698–3706, 2014.

1209 Ye, P., Ding, X., Hakala, J., Hofbauer, V., Robinson, E. S. and Donahue, N. M.: Vapor wall loss  
1210 of semi-volatile organic compounds in a Teflon chamber, *Aerosol Sci. Technol.*, 50(8), 822–834,  
1211 2016.

1212 Zhang, Q., Jimenez, J. L., Canagaratna, M. R., Allan, J. D., Coe, H., Ulbrich, I., Alfarra, M. R.,  
1213 Takami, A., Middlebrook, A. M., Sun, Y. L., Dzepina, K., Dunlea, E., Docherty, K., DeCarlo, P.  
1214 F., Salcedo, D., Onasch, T., Jayne, J. T., Miyoshi, T., Shimono, A., Hatakeyama, S., Takegawa,  
1215 N., Kondo, Y., Schneider, J., Drewnick, F., Borrmann, S., Weimer, S., Demerjian, K., Williams,  
1216 P., Bower, K., Bahreini, R., Cottrell, L., Griffin, R. J., Rautiainen, J., Sun, J. Y., Zhang, Y. M. and  
1217 Worsnop, D. R.: Ubiquity and dominance of oxygenated species in organic aerosols in  
1218 anthropogenically-influenced Northern Hemisphere midlatitudes, *Geophys. Res. Lett.*, 34(13),  
1219 L13801, 2007.

1220 Zhang, Q. J., Beekmann, M., Freney, E., Sellegri, K., Pichon, J. M., Schwarzenboeck, A.,  
1221 Colomb, A., Bourrienne, T., Michoud, V. and Borbon, A.: Formation of secondary organic  
1222 aerosol in the Paris pollution plume and its impact on surrounding regions, *Atmos. Chem. Phys.*,  
1223 15(24), 13973–13992, 2015.

1224 Zhao, B., Wang, S., Donahue, N. M., Jathar, S. H., Huang, X., Wu, W., Hao, J. and Robinson, A.  
1225 L.: Quantifying the effect of organic aerosol aging and intermediate-volatility emissions on  
1226 regional-scale aerosol pollution in China, *Sci. Rep.*, 6, 28815, 2016a.

1227 Zhao, Y., Hennigan, C. J., May, A. A., Daniel, S., Gouw, J. A. D., Gilman, J. B., Kuster, W. C.  
1228 and Robinson, A. L.: Intermediate-Volatility Organic Compounds: A Large Source of Secondary  
1229 Organic Aerosol, *Environ. Sci. Technol.*, 48(23), 13743–13750, 2014.

1230 Zhao, Y., Nguyen, N. T., Presto, A. A., Hennigan, C. J., May, A. A. and Robinson, A. L.:  
1231 Intermediate Volatility Organic Compound Emissions from On-Road Gasoline Vehicles and

1232 Small Off-Road Gasoline Engines, *Environ. Sci. Technol.*, 50(8), 4554–4563, 2016b.

1233 Zhao, Y., Saleh, R., Saliba, G., Presto, A. A., Gordon, T. D., Drozd, G. T., Goldstein, A. H.,  
1234 Donahue, N. M. and Robinson, A. L.: Reducing secondary organic aerosol formation from  
1235 gasoline vehicle exhaust, *Proc. Natl. Acad. Sci. U. S. A.*, 114(27), 6984–6989, 2017.

1236